Variational approach for the multiscale modeling of an estuarian river. Part 1 : Derivation and numerical approximation of a 2D horizontal model

Mohamed Amara, Daniela Capatina, David Trujillo

INSTITUT NATIONAL DE RECHERCHE EN INFORMATIQUE ET EN AUTOMATIQUE

Variational approach for the multiscale modeling of an estuarian river. Part 1 : Derivation and numerical approximation of a 2D horizontal model

Mohamed Amara — Daniela Capatina — David Trujillo

N° 6742

November 2008

Thème NUM

Rapport de recherche

ISSN 0249-6399 ISRN INRIA/RR--6742--FR+ENG

INSTITUT NATIONAL
DE RECHERCHE
EN INFORMATIQUE
ET EN AUTOMATIQUE

INRIA

centre de recherche
BORDEAUX - SUD OUEST

Variational approach for the multiscale modeling of an estuarian river. Part 1 : Derivation and numerical approximation of a 2D horizontal model

Mohamed Amara* , Daniela Capatina † , David Trujillo†

Thème NUM — Systèmes numériques
Équipes-Projets CONCHA

Rapport de recherche n° 6742 — November 2008 — 30 pages

Abstract: The paper is devoted to the 2D hydrodynamical modeling and numerical approximation of an estuarian river flow. A new 2D horizontal model is derived and analyzed as a conforming approximation of the 3D time-discretized problem. It provides the three-dimensional velocity field as well as the pressure, which remains an unknown of the problem. Thanks to the framework of weak formulations, we avoid any closure problem usually encountered in the shallow water system and we can next employ finite elements for the approximation of the 2D model. The discrete problem is shown to be well-posed and finally, numerical tests are presented. The developed code is validated by means of comparisons with the classical shallow water model as well as with measured data.

Key-words: shallow water, 2D hydrodynamical modeling, mixed variational formulations, finite elements

* LMA-UPPA-INRIA-Bordeaux-Sud-Ouest-MAGIC3D
† LMA-UPPA-INRIA-Bordeaux-Sud-Ouest-CONCHA

Centre de recherche INRIA Bordeaux – Sud Ouest
Domaine Universitaire - 351, cours de la Libération 33405 Talence Cedex
Téléphone : +33 5 40 00 69 00

Approche varitionnelle pour la modélisation multi-échelle d'un estuaire: Partie 1: Obtention et approximation numérique d'un modèle 2D horizontal

Résumé : Ce travail est consacré à la modélisation hydrodynamique 2D et à l'approximation numrique de l'estuaire d'un fleuve. Un nouveau modèle 2D horizontal est obtenu et analysé en écrivant une approximation conforme du problème de Navier-Stokes 3D instationnaire. Ce modèle 2D fournit une vitesse tridimensionnelle et le champ de pression est considérée comme une inconnue à part entière. Contrairement au moèle de Saint-Venant aucune équation de fermeture n'est ici nécessaire. La résolution numrique est effectuèe par éléments finis et nous montrons que le problème discret est bien posé. Pour finir, nous présentons des exemples numériques dans lesquel nous faisons des comparaisons avec le modèle classique de Saint-Venant et avec des mesures de terrain.

Mots-clés : Saint-Venant, modélisation hydrodynamique 2D, formulation variationnelle mixte, éléments finis

1 Introduction

The numerical simulation of estuarian river flows plays an important role in many environmental applications (such as overflows, pollutant transport, sedimentation phenomena etc). Besides, many research projects in animal biology necessitate a fine knowledge of the river's hydrodynamics. A realistic model should take into account, at least near the river's estuary, the tide effects, the salinity, the temperature of the water etc. Due to the huge computational cost, a realistic two-phase (fresh / salted water) 3D model cannot be employed on the whole length of the river. Therefore it is interesting to dispose of simpler (2D or 1D) models, to be implemented on adequated regions of the river and then to be coupled in order to get a satisfying numerical global solution.

Several 2D and 1D hydrodynamical models of shallow water type exist in the literature and have been largely used in hydraulics (cf. for instance [11]). In order to derive them, one usually supposes that the pressure is hydrostatic and neglects the vertical velocity in 2D, respectively the vertical and the transversal velocities in 1D. The simplified models are then obtained by integrating the 3D Navier-Stokes equations over a water column in 2D, respectively over a transversal section in 1D. However, their mathematical justification is rather heuristic. Indeed, the closure of the integrated system of equations is achieved through the modeling of a friction term by means of empirical formulae (Manning-Strickler, Chézy etc.); sometimes, a viscous term is also added.

Recent advances have been made in the derivation of shallow water equations, all of them based on asymptotic analysis. One may cite the work of Gerbeau and Perthame [9], which avoids the closure problem for a 1D viscous shallow water system; for simple boundary conditions and a simple geometry, they introduce a friction term without any empirical formula and justify the 1D model by means of an asymptotic analysis of the dimensionless 2D Navier-Stokes equations. Ferrari and Saleri [8] extended this approach to the 2D case including a slowly varying topography and an atmospheric pressure term.

Our goal is the derivation of multidimensional hydrodynamical models, their approximation (with respect to time and space) and their coupling with the automatic determination of the 3D, 2D and 1D computing zones.

We start from the physical 3D model, based on the instationary Navier-Stokes equations and taking into account the Coriolis force, the wind force, the atmospheric pressure, the tide effects and the friction at the bottom. Its time discretization leads to a nonlinear problem, which is next written in mixed variational form. The framework of variational formulations then yields 2D horizontal, 2D vertical and 1D models, obtained from the time-discretized 3D problem by means of a projection method. All the lower-dimensional models provide the three-dimensional velocity and the pressure, which remains an unknown of the problem. The key point is that we thus obtain hierarchical models, that is the 1D problem is a conforming approximation of the 2D horizontal, respectively vertical models, which are both conforming approximations of the 3D one. Moreover, the variational approach naturally avoids any closure problem that one usually encounters in the shallow water system and yields *a priori* and *a posteriori* error estimates between the 3D model and any of its lower-dimensional approximations. *A posteriori* indicators between the discrete models show us how to couple them in a natural way.

The present paper is devoted to the 2D horizontal model only. The 2D vertical and 1D models, as well as the error bounds and an adaptive coupling strategy will be presented in forthcoming papers *(Part II : Derivation and numerical approximation of 2D vertical and 1D models,* respectively *Part III : Adaptive coupling of hydrodynamical models through a posteriori estimators*) .

For the clarity of the paper, let us succinctly present the main features of the 2D horizontal model. The projection subspaces are chosen by specifying the dependence on z of the unknown functions. Thus, if $Z_B(x,y)$ denotes the bottom's elevation, $h(t,x,y)$ the water's elevation and p_S the pressure on the free surface, then the dynamic pressure is looked for as $p_S+(Z_B+h-z)P(t,x,y)$ and the velocity as $(u_1(t,x,y),\, u_2(t,x,y),\, u_3(t,x,y,z))^t$ with $u_3 = u_1\partial_1 Z_B + u_2\partial_2 Z_B+(z-Z_B)U_3(t,x,y)$. Hence at each time-step the unknowns are, besides the height of water h : P, $\mathbf{u}_H = (u_1,u_2)^t$ and U_3, functions of (x,y) in the domain defined by $h>0$. If we place ourselves in the same framework as for the shallow water equations (that is, no vertical velocity u_3 and hydrostatic pressure), then our 2D model reduces to :

$$\begin{aligned}
\frac{\partial h}{\partial t} + div\,(h\mathbf{u}_H) &= 0,\\
\frac{\partial (h\mathbf{u}_H)}{\partial t} + div\,(h\mathbf{u}_H\otimes\mathbf{u}_H) + \frac{\mu}{\rho}\mathbf{curl}(hcurl\mathbf{u}_H) - \frac{h}{2}\nabla\left|\mathbf{u}_H\right|^2 &+\\
\frac{c_B}{\rho}\sqrt{1+\left|\nabla Z_B\right|^2}\mathbf{u}_H - hf\mathbf{u}_H^{\perp} &\\
= -gh\nabla(Z_B+h) + \mathbf{w} &
\end{aligned}$$

where $\mathbf{u}_H^{\perp} = (-u_2,u_1)^t$, $\mathbf{w}$ represents the wind's effect, c_B the friction coefficient on the bottom, f the earth's angular velocity and μ, ρ respectively denote the viscosity and the density of the fluid. So one can note that it mainly differs from the shallow water system through the friction term.

We have carried out a mathematical analysis of the time-discretized 2D model, at the continuous and discrete levels. Two situations are to be envisaged : the degenerate case where the water's elevation may vanish on the riverbanks, and the non degenerate one corresponding to h strictly positive. We have established the well-posedness of the continuous nonlinear problem in both cases. However, due to the restrictive hypotheses and to the difficulties related to weighted Hilbert spaces involved in the degenerate case, we only present the space discretization in the non degenerate one. We propose a simple, low-order conforming approximation, which uses P_0 finite elements for the pressure, $(P_1)^2$- continuous elements for the horizontal velocities and P_1- continuous elements enriched with bubbles for the vertical velocity U_3. The proof of the well-posedness of the discrete problem makes use of Brouwer's theorem together with Babuška's inf-sup condition.

The paper is organized as follows. Section 2 is devoted to the introduction of the 3D model, whose time-discretized version is next shown to be well-posed. In Section 3, we derive and then analyse the time-discretized 2D horizontal problem. We also deduce the corresponding boundary value problem and compare it to the classical shallow water equations. The finite element approximation of the new 2D model is discussed in Section 4, where we prove that the discrete problem has a unique solution. Finally, the last section is devoted to the validation of the 2D code. Numerical tests achieved with a realistic case (Adour

estuarian river in France), as well as a comparison with the 2D shallow water system are presented. As expected, our model is more appropriate in the regions of the river where the bottom varies, since it computes a vertical velocity which is simply supposed to be null in the shallow water approach.

2 Three-dimensional physical problem

2.1 Notations and problem setting

Let us begin by introducing some notations. In what follows, we agree to write the vector functions in bold letters and to denote the vector product by $\wedge$. For any 3D vector field $\mathbf{v} = (v_1, v_2, v_3)^t$ we denote :

$$div\mathbf{v} = \partial_1 v_1 + \partial_2 v_2 + \partial_3 v_3, \quad \mathbf{curlv} = (\partial_2 v_3 - \partial_3 v_2, \partial_3 v_1 - \partial_1 v_3, \partial_1 v_2 - \partial_2 v_1)^t,$$

while for a 2D vector field $\mathbf{v} = (v_1, v_2)^t$ we put :

$$\mathbf{v}^\perp = (-v_2, v_1)^t, \quad div\mathbf{v} = \partial_1 v_1 + \partial_2 v_2, \quad curl\mathbf{v} = \partial_1 v_2 - \partial_2 v_1.$$

We agree to denote by the letter c any positive constant independent of the time and space discretization.

Let $\Omega_F(t) \subset \mathbb{R}^3$ denote the moving domain occupied by the fluid, of boundary decomposed as follows :

$$\partial\Omega_F(t) \quad = \quad \Gamma_B(t) \cup \Gamma_S(t) \cup \Gamma_I(t)$$

where $\Gamma_B(t)$ is the riverbed, $\Gamma_S(t)$ the free surface and $\Gamma_I(t)$ the inflow or outflow boundary.

We agree to denote by $Z_B(x, y)$ the elevation of the bottom, given by the bathymetry and defined on a maximal domain $\Sigma \subset \mathbb{R}^2$. Let us also introduce the height of the water $h(t, x, y)$ and the 2D domain $\Sigma_F(t) \subset \Sigma$, defined at each instant by $h > 0$:

$$\Sigma_F(t) = \{(x, y);\ h(t, x, y) > 0\}, \quad \Sigma_F(t) \subset \Sigma,\ \forall t > 0.$$

One can see $\Sigma_F(t)$ as the horizontal projection of the free surface $\Gamma_S(t)$ on Σ. Then we have

$$\begin{aligned} \Omega_F(t) &= \{(x, y, z);\ (x, y) \in \Sigma_F(t),\ \ Z_B < z < Z_B + h\}, \\ \Gamma_S(t) &= \{(x, y, z);\ (x, y) \in \Sigma_F(t),\ \ z = Z_B + h\}. \end{aligned}$$

We neglect the temperature and the salinity of the water and we consider only the hydrodynamical aspects. The physical problem is described by the instationary incompressible Navier-Stokes equations in $\Omega_F(t)$. We suppose that the density of the water is constant and we take into account the gravity and Coriolis forces, which leads to the following governing equations :

$$\begin{cases} div\mathbf{u} = 0 \\ \rho \dfrac{\partial \mathbf{u}}{\partial t} + \rho\mathbf{u} \cdot \nabla\mathbf{u} - \mu\Delta\mathbf{u} + \nabla\widetilde{p} - \rho\mathbf{f} \wedge \mathbf{u} = \rho\mathbf{g}. \end{cases}$$

The unknowns are the velocity $\mathbf{u}$ and the pressure $\widetilde{p}$, while the density ρ, the viscosity μ, the gravity force $\mathbf{g} = (0, 0, -g)$, the earth's rotation velocity $\mathbf{f} = (0, 0, f)$ are given constants. By means of the formulae

$$\begin{aligned} -\Delta\mathbf{u} &= \mathbf{curl}(\mathbf{curl}\,\mathbf{u}) - \nabla(div\mathbf{u}), \\ \mathbf{u}\cdot\nabla\mathbf{u} &= \mathbf{curlu}\wedge\mathbf{u} + \frac{1}{2}\nabla\left|\mathbf{u}\right|^2, \end{aligned}$$

the momentum equation can be equivalently written as follows :

$$\rho\frac{\partial\mathbf{u}}{\partial t} + \rho\mathbf{curlu}\wedge\mathbf{u} + \mu\mathbf{curl}(\mathbf{curl}\,\mathbf{u}) + \nabla p - \rho\mathbf{f}\wedge\mathbf{u} = \rho\mathbf{g}$$

where p now represents the dynamic pressure, defined by $p = \widetilde{p} + \dfrac{\rho}{2}\left|\mathbf{u}\right|^2$.

To the previous equations, we add the initial condition $\mathbf{u}(0) = \mathbf{u}_0$ as well as boundary conditions. In our work it is worth noting the originality of the conditions considered on the free surface : we impose the pressure and the tangential stresses, while usually in the shallow water modeling the vertical velocity is set to zero. We also impose a friction and an impermeability condition on the bottom, which finally yields the following set of boundary conditions :

$$\left\{\begin{array}{ccc} \mathbf{u}\cdot\mathbf{n} = 0\ , \quad \mu\mathbf{curlu}\wedge\mathbf{n} = -c_B\mathbf{u} & & \text{on } \Gamma_B(t) \\ p = p_S, \quad \mu\mathbf{curlu}\wedge\mathbf{n} = \mathbf{w} & & \text{on } \Gamma_S(t) \\ \mathbf{u}\cdot\mathbf{n} = k, \quad \mu\mathbf{curlu}\wedge\mathbf{n} = \mathbf{w} & & \text{on } \Gamma_I(t) \end{array}\right. \tag{1}$$

where $\mathbf{n}$ is the outword unit normal vector to $\partial\Omega_F(t)$, p_S, k, $\mathbf{w}$ are given functions and the friction coefficient $c_B \geq 0$ is a given constant. The data $\mathbf{w}$ is related to the wind's force on the free surface, respectively to the tide on the estuarine boundary; $p_S$represent the surface pressure and$k$ the inflow or the outflow.

Finally, we close the system by adding the free surface equation (cf. for instance [9]) :

$$\frac{\partial h}{\partial t} + \sum_{i=1}^{2} u_i\partial_i(Z_B + h) = u_3 \quad \text{on } \Gamma_S(t), \tag{2}$$

together with an initial condition $h(0) = h_0$.

The three-dimensional problem in the unknowns $(h, \mathbf{u}, p)$ is next time-discretized by means of an implicit Euler's scheme; we choose here :

$$\frac{h - h^n}{\Delta t} + \sum_{i=1}^{2} u_i^n\partial_i(Z_B + h) = u_3^n \quad \text{on } \Gamma_S(t^n),$$

$$\left\{\begin{array}{c} div\mathbf{u} = 0 \\ \dfrac{\rho}{\Delta t}(\mathbf{u} - \mathbf{u}^n) + \rho\mathbf{curlu}\wedge\mathbf{u} + \mu\mathbf{curl}(\mathbf{curlu}) - \rho\mathbf{f}\wedge\mathbf{u} + \nabla p = \rho\mathbf{g} \end{array}\right. \quad \text{in } \Omega_F(t^{n+1}). \tag{3}$$

We agree to denote in what follows the domain occupied by the fluid at t^{n+1} (defined by the condition $h > 0$) by Ω_F, its boundary by $\partial\Omega_F = \Gamma_B \cup \Gamma_S \cup \Gamma_I$ and k^{n+1}, $\mathbf{w}^{n+1}$, p_S^{n+1} by k, $\mathbf{w}$, p_S respectively.

We assume in the sequel that Ω_F is bounded and Lipschitz-continuous. In order to prove the well-posedness of the 3D time-discretized problem, we also need to suppose that Ω_F has either a polyhedral boundary or a sufficiently smooth boundary (for instance, $C^{1,1}$).

2.2 Analysis of the semi-discretized problem

In this paragraph we prove that, at any t^{n+1}, the nonlinear boundary value problem (3) is well-posed. For this purpose, we write it in weak form and then apply a variant of Brouwer's theorem (cf. for instance [10]) to show existence and, under certain hypotheses, uniqueness of the solution. We suppose that the boundary data satisfy at any time step the following regularity :

$$k \in L^2(\Gamma_I), \quad \overline{p}_S \in H^{1/2}(\partial\Omega_F), \quad \mathbf{w}\wedge\mathbf{n} \in \mathbf{H}^{1/2}_{00}(\Gamma_I\cup\Gamma_S)$$

where $\overline{p}_S$ represents a continuous extension of p_S on the whole boundary (i.e. $p_S = (\overline{p}_S)_{/\Gamma_S}$).

Let us define the Hilbert spaces :

$$\begin{aligned} M &= L^2(\Omega_F), \\ \mathbf{H}(div,\mathbf{curl};\Omega_F) &= \left\{\mathbf{v}\in\mathbf{L}^2(\Omega_F);\ div\mathbf{v}\in L^2(\Omega_F),\ \mathbf{curlv}\in\mathbf{L}^2(\Omega_F)\right\}, \\ \mathbf{X} &= \left\{\mathbf{v}\in\mathbf{H}(div,\mathbf{curl};\Omega_F);\ \mathbf{v}_{|\Gamma_B}\in\mathbf{L}^2(\Gamma_B)\right\}. \end{aligned}$$

The spaces M and $\mathbf{X}$ are endowed with the following norms :

$$\begin{aligned} \|q\|_M &= \|q\|_{0,\Omega_F} = \left(\int_{\Omega_F} q^2 d\Omega\right)^{1/2}, \\ \|\mathbf{v}\|^2_{\mathbf{X}} &= \left(\frac{1}{\Delta t}\|\mathbf{v}\|^2_{0,\Omega_F} + \|div\mathbf{v}\|^2_{0,\Omega_F} + \|\mathbf{curlv}\|^2_{0,\Omega_F} + \|\mathbf{v}\|^2_{0,\Gamma_B}\right)^{1/2}. \end{aligned}$$

We also introduce :

$$\begin{aligned} \mathbf{X}^0 &= \{\mathbf{v}\in\mathbf{X};\ \mathbf{v}\cdot\mathbf{n} = 0 \text{ on } \Gamma_B\cup\Gamma_I\}, \\ \mathbf{X}^* &= \{\mathbf{v}\in\mathbf{X};\ \mathbf{v}\cdot\mathbf{n} = 0 \text{ on } \Gamma_B,\ \mathbf{v}\cdot\mathbf{n} = k \text{ on } \Gamma_I\}. \end{aligned}$$

Let us comment the necessity of imposing the condition $\mathbf{v}\in\mathbf{L}^2(\Gamma_B)$ in the definition of the space $\mathbf{X}$. For that, let D be a sufficiently smooth bounded domain and Υ_1, Υ_2 a partition of its boundary. If $\mathbf{v}\in\mathbf{H}(div,\mathbf{curl};D)$ satisfies $\mathbf{v}\cdot\mathbf{n} = 0$ on Υ_1 and $\mathbf{v}\wedge\mathbf{n} = \mathbf{0}$ on Υ_2, then one can establish similarly to [7] that $\mathbf{v}\in\mathbf{L}^2(\partial D)$. However, in our case, a boundary condition of such type is missing on the free surface, where the pressure is given instead. Hence, for a given $\mathbf{v}\in\mathbf{H}(div,\mathbf{curl};\Omega_F)$ satisfying $\mathbf{v}\cdot\mathbf{n} = 0$ on $\Gamma_B\cup\Gamma_I$, one can only deduce that $\mathbf{v}\in\mathbf{L}^2_{loc}(\Gamma_B\cup\Gamma_I)$, wherefrom the definition of the space $\mathbf{X}$.

From now on, we shall assume that at any t^{n+1} the space $\mathbf{X}^0$ satisfies the conditions :
(H1) $\mathbf{X}^0$ is continuously embedded in $\mathbf{L}^4(\Omega_F)$ and compactly embedded in $\mathbf{L}^2(\Omega_F)$;
(H2) $tr(\mathbf{X}^0)$ is compactly embedded in $\mathbf{L}^2(\Gamma_S)$, where

$$tr(\mathbf{X}^0) = \left\{\mathbf{\Theta}\in\mathbf{H}^{-1/2}(\Gamma_S);\ \exists\mathbf{v}\in\mathbf{X}^0,\ \mathbf{v} = \mathbf{\Theta} \text{ on } \Gamma_S\right\}.$$

Note that, thanks to Kondrasov's theorem, both compact embeddings hold if $\mathbf{X}^0\subset\mathbf{H}^s(\Omega_F)$ with $s > 1/2$. If, moreover, $s\geq 3/4$ then Sobolev's theorem also ensures the first assertion.

Remark 1. *One may also think of imposing in (1)* $\mathbf{u}\cdot\mathbf{n}$ *instead of the dynamic pressure on the free surface. In this case, supposing that the domain* Ω_F *is a convex polyhedron (or has a* $C^{1,1}$ *boundary), one can show following [7] or [10] that the new space associated with the velocity is continuously embedded in* $\mathbf{H}^1(\Omega_F)$*, so the two previous hypotheses are fulfilled. Moreover, as we shall see further, taking into account this new boundary condition yields a perfectly determined vertical velocity in the 2D model.*

Problem (3) can now be written in weak form as follows :

$$\left\{\begin{array}{l} Find\ (\mathbf{u},p)\in \mathbf{X}^*\times M \\ \forall \mathbf{v}\in \mathbf{X}^0,\quad A(\mathbf{u};\mathbf{u},\mathbf{v})+B(p,\mathbf{v})=F^n(\mathbf{v}) \\ \forall q\in M,\quad B(q,\mathbf{u})=0, \end{array}\right. \tag{4}$$

where

$$\begin{aligned} A(\mathbf{w};\mathbf{u},\mathbf{v}) &= A_0(\mathbf{u},\mathbf{v})+A_1(\mathbf{w};\mathbf{u},\mathbf{v}), \\ A_0(\mathbf{u},\mathbf{v}) &= \int_{\Omega_F}\frac{\rho}{\Delta t}\mathbf{u}\cdot\mathbf{v}\,d\Omega+\int_{\Omega_F}\mu\mathbf{curlu}\cdot\mathbf{curlv}\,d\Omega+\int_{\Gamma_B}c_B\mathbf{u}\cdot\mathbf{v}\,d\Gamma \\ &\quad -\int_{\Omega_F}\rho(\mathbf{f}\wedge\mathbf{u})\cdot\mathbf{v}\,d\Omega, \\ A_1(\mathbf{w};\mathbf{u},\mathbf{v}) &= \int_{\Omega_F}\rho(\mathbf{curlu}\wedge\mathbf{w})\cdot\mathbf{v}\,d\Omega, \\ B(p,\mathbf{v}) &= -\int_{\Omega_F}p\,div\mathbf{v}\,d\Omega, \\ F^n(\mathbf{v}) &= \int_{\Omega_F}\rho(\frac{1}{\Delta t}\mathbf{u}^n+\mathbf{g})\cdot\mathbf{v}\,d\Omega+<\mathbf{v}\wedge\mathbf{n},\mathbf{w}\wedge\mathbf{n}>_{\Gamma_S\cup\Gamma_I}-<\mathbf{v}\cdot\mathbf{n},\overline{p}_S>_{\partial\Omega_F} \end{aligned}$$

and where $<\cdot,\cdot>_\Gamma$ stands for the duality product between $H^{1/2}_{00}(\Gamma)$ and $H^{-1/2}(\Gamma)$. Thanks to the hypothesis *(H1)*, the nonlinear form $A_1(\cdot;\cdot,\cdot)$ is well-defined since $\mathbf{curlu}\in\mathbf{L}^2(\Omega_F)$ and $\mathbf{v},\mathbf{w}\in\mathbf{L}^4(\Omega_F)$ and it satisfies :

$$A_1(\mathbf{w};\mathbf{u},\mathbf{v})\le\rho\,\|\mathbf{curlu}\|_{0,\Omega_F}\,\|\mathbf{v}\|_{\mathbf{L^4(\Omega_F)}}\,\|\mathbf{w}\|_{\mathbf{L^4(\Omega_F)}}\le\rho c_1^2\,\|\mathbf{u}\|_{\mathbf{X}}\,\|\mathbf{v}\|_{\mathbf{X}}\,\|\mathbf{w}\|_{\mathbf{X}},$$

where $c_1(\Delta t)$ is the norm of the identity operator $\mathcal{I}:(\mathbf{X}^0,\|\cdot\|_{\mathbf{X}})\to(\mathbf{L}^4(\Omega_F),\|\cdot\|_{\mathbf{L^4(\Omega_F)}})$. The bilinear forms $A_0(\cdot,\cdot)$ and $B(\cdot,\cdot)$ are clearly continuous. The trace theorems in $\mathbf{H}(div,\Omega_F)$, respectively $\mathbf{H}(\mathbf{curl},\Omega_F)$ state that :

$$\begin{aligned} \|\mathbf{v}\wedge\mathbf{n}\|_{-1/2,\partial\Omega_F} &\le (\|\mathbf{v}\|^2_{0,\Omega_F}+\|\mathbf{curlv}\|^2_{0,\Omega_F})^{1/2}, \\ \|\mathbf{v}\cdot\mathbf{n}\|_{-1/2,\partial\Omega_F} &\le (\|\mathbf{v}\|^2_{0,\Omega_F}+\|div\mathbf{v}\|^2_{0,\Omega_F})^{1/2}, \end{aligned}$$

which imply the continuity of $F^n(\cdot)$ with a constant $c_2(\Delta t)$ satisfying :

$$c_2(\Delta t)\le\max\left\{\frac{\rho\,\|\mathbf{u}^n\|_{0,\Omega_F}}{\sqrt{\Delta t}},C\right\}$$

where C depends on the data as follows :

$$C\le c(\|\rho\mathbf{g}\|_{0,\Omega_F}+\|\mathbf{w}\wedge\mathbf{n}\|_{1/2,\Gamma_S\cup\Gamma_I}+\|\overline{p}_S\|_{1/2,\partial\Omega_F}).$$

Then we can establish :

Theorem 1. *Problem (4) has at least one solution. If moreover*

$$c_2 \quad < \quad \frac{1}{2\rho}\left(\frac{c_3}{c_1}\right)^2,$$

then the solution is unique.

Proof. We make use of a classical result which can be found in [10], p.280 and which is a consequence of Brouwer's fixed point theorem.

More precisely, we first show that $B(\cdot,\cdot)$ satisfies an inf-sup condition, therefore it is sufficient to study the problem

$$\left\{\begin{array}{c} Find\ \mathbf{u} \in \mathbf{V}^* \\ \forall \mathbf{v} \in \mathbf{V}^0, \quad A(\mathbf{u};\mathbf{u},\mathbf{v}) = F^n(\mathbf{v}) \end{array}\right. \tag{5}$$

instead of (4), where now

$$\begin{array}{rcl} \mathbf{V} & = & \{\mathbf{v} \in \mathbf{X};\ div\mathbf{v} = 0 \text{ in } \Omega_F\}, \\ \mathbf{V}^0 & = & \mathbf{V} \cap \mathbf{X}^0 = KerB, \\ \mathbf{V}^* & = & \mathbf{V} \cap \mathbf{X}^*. \end{array}$$

In order to prove the inf-sup condition we apply Fortin's trick, which consists in building a continuous operator $\mathcal{R} : M \to \mathbf{X}^0$ satisfying $B(q,\mathcal{R}q) = \|q\|_M^2$, $\forall q \in M$. For this purpose, with any $q \in M$ we associate the auxiliary problem :

$$\left\{\begin{array}{cc} -\Delta w = q & \text{in } \Omega_F \\ \partial_n w = 0 & \text{on } \partial\Omega_F \setminus \Sigma \\ w = 0 & \text{on } \Sigma_F. \end{array}\right.$$

Thanks to the assumed regularity of Ω_F, the regularity of the previous elliptic problem ensures (cf. [12]) that $w \in H^{1+a}(\Omega_F)$ with $a > 1/2$ and

$$\|w\|_{1+a,\Omega_F} \leq c\,\|q\|_{0,\Omega_F},$$

where the constant c depends on Ω_F. Then by putting $\mathcal{R}q = \nabla w$ we obviously obtain $B(q,\mathcal{R}q) = \|q\|_M^2$ and also : $(\mathcal{R}q)_{/\partial\Omega_F} \in \mathbf{L}^2(\partial\Omega_F)$, $div(\mathcal{R}q) = -q$, $\mathbf{curl}(\mathcal{R}q) = \mathbf{0}$ and $\mathcal{R}q \cdot \mathbf{n} = 0$ on $\Gamma_I \cup \Gamma_B$ by construction of the operator $\mathcal{R}$. It follows that $\mathcal{R}q \in \mathbf{X}^0$ and moreover, by means of the trace theorem one has :

$$\|\mathcal{R}q\|_{0,\Gamma_B} = \|\nabla w\|_{0,\Gamma_B} \leq c\,\|w\|_{1+a,\Omega_F}.$$

Therefore, $\|\mathcal{R}q\|_{\mathbf{X}} \leq \frac{c}{\sqrt{\Delta t}}\,\|q\|_M$ and finally :

$$\inf_{q\in M}\sup_{\mathbf{v}\in\mathbf{X}^0}\frac{B(q,\mathbf{v})}{\|\mathbf{v}\|_{\mathbf{X}}\,\|q\|_M} \geq c\sqrt{\Delta t}.$$

Then the Babuška-Brezzi theorem ensures that for each $\mathbf{u}$ solution of (5), there exists a unique $p \in M$ such that the pair $(\mathbf{u},p)$ is solution of the initial mixed problem (4).

We next consider the nonlinear problem (5) and we notice that

$$A(\mathbf{v};\mathbf{v},\mathbf{v}) = A_0(\mathbf{v},\mathbf{v}) \geq c_3\,\|\mathbf{v}\|_{\mathbf{X}}^2, \quad \forall \mathbf{v} \in \mathbf{V}^0$$

with $c_3 = \min\{\mu, c_B, \rho\}$.

Note that the space $\mathbf{V}^0$ is separable as a subspace of $\mathbf{L}^2(\Omega_F)$ and moreover, $\mathbf{V}^0 \cap D(\overline{\Omega}_F)^3$ is a dense subspace of $\mathbf{V}^0$. Therefore, it is sufficient to prove (cf. [10]) that for all $\mathbf{v} \in \mathbf{V}^0 \cap D(\overline{\Omega}_F)^3$, $A_1(\cdot;\cdot,\mathbf{v})$ is sequentially weakly-continuous on $\mathbf{V}^0$ in order to obtain the existence of a solution to problem (5). For this purpose, we write thanks to an integration by parts that

$$A_1(\mathbf{u};\mathbf{u},\mathbf{v}) = -\int_{\Omega_F} \rho v_{i,j} u_i u_j d\Omega + \int_{\Gamma_S} \rho \mathbf{v}\cdot\mathbf{u}\mathbf{u}\cdot\mathbf{n} d\Gamma - \frac{1}{2}\int_{\Gamma_S} \rho \mathbf{v}\cdot\mathbf{n}\,|\mathbf{u}|^2\, d\Gamma, \quad \forall \mathbf{u} \in \mathbf{V}^0.$$

Thanks to the initial assumptions on the space $\mathbf{X}^0$, notably to the compact embeddings in $\mathbf{L}^2(\Omega_F)$ and $\mathbf{L}^2(\Gamma_S)$, and to the fact that $v_{i,j} \in L^\infty(\Omega_F)$, one deduces that $w - \lim_{m\to\infty} \mathbf{u}_m = \mathbf{u}$ in $\mathbf{V}^0$ implies $w - \lim_{m\to\infty} A(\mathbf{u}_m;\mathbf{u}_m,\mathbf{v}) = A(\mathbf{u};\mathbf{u},\mathbf{v})$.

In conclusion, problem (5) written on the kernel of $B(\cdot,\cdot)$ has at least one solution. The uniqueness is established under the usual hypothesis of small data, that is the norm of the righthand-side operator should be small. So let $\mathbf{u}_1$, $\mathbf{u}_2$ be two solutions of (5) and let us show that $\mathbf{u}_1 = \mathbf{u}_2$. We first write for any $\mathbf{v} \in \mathbf{V}^0$ that :

$$0 = A_0(\mathbf{u}_1 - \mathbf{u}_2, \mathbf{v}) + A_1(\mathbf{u}_1;\mathbf{u}_1 - \mathbf{u}_2,\mathbf{v}) - A_1(\mathbf{u}_1 - \mathbf{u}_2;\mathbf{u}_2,\mathbf{v}).$$

We next take $\mathbf{v} = \mathbf{u}_1 - \mathbf{u}_2$ and use the coercivity of $A_0(\cdot,\cdot)$ and the continuity of $A_1(\cdot;\cdot,\cdot)$ in order to obtain that :

$$c_3 \|\mathbf{u}_1 - \mathbf{u}_2\|^2_{\mathbf{X}} \le \rho c_1^2 \|\mathbf{u}_1 - \mathbf{u}_2\|^2_{\mathbf{X}} \left(\|\mathbf{u}_1\|_{\mathbf{X}} + \|\mathbf{u}_2\|_{\mathbf{X}}\right).$$

Since $A_1(\mathbf{u};\mathbf{u},\mathbf{u}) = 0$, any solution $\mathbf{u}$ of (4) satisfies the estimate $\|\mathbf{u}\|_{\mathbf{X}} \le \frac{c_2}{c_3}$. This leads to :

$$\|\mathbf{u}_1 - \mathbf{u}_2\|^2_{\mathbf{X}} \le \frac{2\rho c_1^2 c_2}{c_3^2} \|\mathbf{u}_1 - \mathbf{u}_2\|^2_{\mathbf{X}}$$

which finally implies that $\mathbf{u}_1 - \mathbf{u}_2 = 0$ if $\frac{2\rho c_1^2 c_2}{c_3^2} < 1$. So the announced result is established. □

Concerning the interpretation of the variational problem in the sense of distributions, one can classically prove that the solution $(\mathbf{u}, p)$ of (4) satisfies the semi-discretized equations (3), together with the boundary conditions (1) on $\partial\Omega_F$(see for instance [2]).

3 2D horizontal model

This section is devoted to the derivation and study of a 2D hydrodynamical model, obtained at any t^{n+1} from (2) and (4) by projection on conveniently chosen subspaces $\mathbf{X}_H \times M_H \subset \mathbf{X} \times M$.

We first consider in subsections 3.1 to 3.3 the general case where the water's height h may vanish on the riverbanks. This complicates the mathematical analysis, since one now deals with degenerate equations and weighted spaces. Finally, the case of strictly positive depth will also be discussed in subsection 3.4.

3.1 Projection spaces and derived model

The 2D horizontal model will be written on the 2D domain $\Sigma_F(t) \subset \Sigma$. Its derivation is achieved under the following hypotheses :
(i) the inflow / outflow boundaries Γ_I are assumed to be vertical;
(ii) the riverbed is described by $z = Z_B(x, y)$, where the data Z_B satisfies :

$$Z_B \quad \in \quad W^{2,\infty}(\Sigma_F).$$

The first assumption *(i)* is neither restrictive nor essential, but it allows an easier presentation of the method. For the sake of simplicity, we also agree to take $\mathbf{w} = \mathbf{0}$ on Γ_I.

It is useful to introduce, at each t^{n+1}: $\partial\Sigma_F = \Upsilon_I \cup \Upsilon_{lat}$ where Υ_I corresponds to the inflow or outflow boundary while Υ_{lat} corresponds to the riverbanks (characterized by $h = 0$).

For a given function $\alpha \geq 0$ and a given domain ω, we define the weighted Hilbert space :

$$L^2(\omega, \alpha) = \left\{ q;\ \int_\omega q^2 \alpha \, d\omega < \infty \right\}$$

endowed with the norm : $\|q\|_{0,\omega,\alpha} = (\int_\omega q^2 \alpha \, d\omega)^{1/2}$. It goes the same way for $H^1(\omega, \alpha)$. Then for given h, we can now introduce the following projection spaces :

$$\begin{aligned}
M_H &= \left\{ q;\ q(x,y,z) = (Z_B + h - z)Q(x,y);\ Q \in L^2(\Sigma_F, h^3) \right\}, \\
\mathbf{X}_H &= \Big\{ (\mathbf{v}_H, v_3)^t ;\ \mathbf{v}_H \in \mathbf{H}(div, curl; \Sigma_F, h) \cap \mathbf{L}^2(\Sigma_F),\ \mathbf{v}_H \cdot \nabla Z_B \in H^1(\Sigma_F, h), \\
&\quad v_3(x,y,z) = \mathbf{v}_H \cdot \nabla Z_B + (z - Z_B)V_3(x,y),\ V_3 \in H^1(\Sigma_F, h^3) \cap L^2(\Sigma_F, h) \Big\}, \\
\mathbf{X}_H^0 &= \{\ \mathbf{v} \in \mathbf{X}_H;\ \mathbf{v}_H \cdot \mathbf{n}_H = 0 \text{ on } \Upsilon_I \},
\end{aligned} \tag{6}$$

where we have put :

$$\mathbf{v}_H = (v_1(x,y), v_2(x,y))^t$$

and where $\mathbf{n}_H$ is the outward normal unit vector to Υ_I. For the simplicity of the presentation, let us also introduce the notation

$$v_B \quad = \quad \mathbf{v}_H \cdot \nabla Z_B.$$

So, the elements of M_H and $\mathbf{X}_H$ are completely determined by the functions Q, $\mathbf{v}_H$ and V_3 which are all independent of the variable z. We also need to introduce the affine spaces :

$$\begin{aligned}
M_H^* &= \left\{ q;\ q(x,y,z) = p_S + (Z_B + h - z)Q(x,y);\ Q \in L^2(\Sigma_F, h^3) \right\}, \\
\mathbf{X}_H^* &= \{\ \mathbf{v} \in \mathbf{X}_H;\ \mathbf{v}_H \cdot \mathbf{n}_H = k_H \text{ on } \Upsilon_I \},
\end{aligned}$$

where $k_H = k_H(x, y)$ represents an approximation of $k(x, y, z)$ on Υ_I, for instance $k_H(x, y) = \dfrac{1}{h} \int_{Z_B}^{Z_B+h} k(x, y, z) dz$.

This choice of subspaces guarantees a conforming approximation with respect to the initial 3D model, as shown in the next proposition. Moreover, we thus recover a vertical velocity and a pressure which are affine with respect to z.

Theorem 2. *One has that* $\mathbf{X}_H^0 \subset \mathbf{X}^0$ *and* $M_H \subset M$.

Proof. The condition $\mathbf{v}\cdot\mathbf{n}=0$ on Γ_B is automatically satisfied by construction of v_3. Indeed, a normal vector to Γ_B is given by $(\partial_1 Z_B, \partial_2 Z_B, -1)^t$ so on the riverbed one has :

$$\mathbf{v}\cdot\mathbf{n} = \mathbf{v}_H\cdot\nabla Z_B - v_3 = 0.$$

Moreover, if $\mathbf{v}\in\mathbf{X}_H^0$ then $\mathbf{v}\in\mathbf{L}^2(\Gamma_B)$ since :

$$\int_{\Gamma_B}\mathbf{v}^2 d\Gamma = \int_{\Sigma_F}\mathbf{v}^2\sqrt{1+|\nabla Z_B|^2}dxdy \le c\int_{\Sigma_F}\mathbf{v}_H^2 dxdy < \infty.$$

Next, one can remark that the outward normal unit vector to Γ_I is $\mathbf{n}=(\mathbf{n}_H,0)^t$, so for any $\mathbf{v}\in\mathbf{X}_H^0$ it follows that $\mathbf{v}\cdot\mathbf{n}=0$ on Γ_I. Finally, let us notice that for any $\mathbf{v}\in\mathbf{X}_H$, $q\in M_H$ one has :

$$\begin{aligned}
\int_{\Omega_F}|\mathbf{v}|^2 d\Omega &= \int_{\Sigma_F} h\left(|\mathbf{v}_H|^2 + (v_B+\frac{h}{2}V_3)^2 + \frac{h^2}{12}V_3^2\right)dxdy,\\
\int_{\Omega_F}|\mathbf{curl}\mathbf{v}|^2 d\Omega &= \int_{\Sigma_F} h\left((curl\mathbf{v}_H)^2 + \left|\nabla v_B + \frac{h}{2}\nabla V_3\right|^2 + \frac{h^2}{12}|\nabla V_3|^2\right)dxdy,\\
\int_{\Omega_F}|div\mathbf{v}|^2 d\Omega &= \int_{\Sigma_F} h(div\mathbf{v}_H + V_3)^2 dxdy,\\
\int_{\Omega_F} q^2 d\Omega &= \frac{1}{3}\int_{\Sigma_F} h^3 Q^2 dxdy \qquad (7)
\end{aligned}$$

and the statement is established. □

Concerning the choice of the space $\mathbf{X}_H$, let us highlight the following points :

- One could think of simplifying the definition (6) of $\mathbf{X}_H$ by imposing

  $$\mathbf{v}_H \in \mathbf{H}^1(\Sigma_F,h)\cap\mathbf{L}^2(\Sigma_F).$$

  However, this is not justified in the case of a flat bottom (characterized by $\nabla Z_B=\mathbf{0}$), as in this case (6) only implies that $\mathbf{v}_H\in\mathbf{H}(div,curl;\Sigma_F,h)\cap\mathbf{L}^2(\Sigma_F)$.

- If one chooses to impose $\mathbf{u}\cdot\mathbf{n}=U(x,y)$ rather than the dynamic pressure p_S on the free surface $\Gamma_S(t)$, then the inclusion $\mathbf{X}_H^0\subset\mathbf{X}^0$ yields a vertical velocity which is completely determined in terms of $\mathbf{u}_H$:

  $$u_3 = \mathbf{u}_H\cdot\nabla Z_B + (z-Z_B)U_3, \quad \text{with} \quad U_3 = \frac{\mathbf{u}_H\cdot\nabla h - U}{h}.$$

Let us now proceed with the derivation of the 2D horizontal model. We first deduce the equation satisfied by h from the free surface equation (2), by taking the 3D velocity in $\mathbf{X}_H$. This leads to

$$\frac{\partial h}{\partial t} + \mathbf{u}_H\cdot\nabla h = hU_3 \quad \text{on } \Sigma,$$

to which we add an initial condition on h. We semi-discretize the previous equation and, at each time step t^{n+1}, we solve for instance :

$$\frac{h-h^n}{\Delta t} + \mathbf{u}_H^n \cdot \nabla h - hU_3^n = 0 \quad \text{on } \Sigma.$$

Next, once h computed we define the computational domain Σ_F by $h > 0$. Then we introduce the spaces $\mathbf{X}_H^0$, M_H associated with the above h and Σ_F and we consider the following conforming approximation of (4) :

$$\left\{ \begin{array}{l} \textit{Find } (\mathbf{u}_{2D}, p_{2D}) \in \mathbf{X}_H^* \times M_H^* \\ \forall \mathbf{v} \in \mathbf{X}_H^0, \quad A(\mathbf{u}_{2D}; \mathbf{u}_{2D}, \mathbf{v}) + B(p_{2D}, \mathbf{v}) = F_H^n(\mathbf{v}) \\ \forall q \in M_H, \quad B(q, \mathbf{u}_{2D}) = 0 \end{array} \right. \tag{8}$$

where

$$\begin{array}{rcl} \mathbf{u}_{2D} & = & (\mathbf{u}_H, u_B + (z - Z_B)U_3)^t, \\ p_{2D} & = & p_S + (Z_B + h - z)P. \end{array}$$

The righthand-side term $F_H^n(\cdot)$ is obtained by replacing $\mathbf{u}^n$ by $\mathbf{u}_{2D}^n$ in $F^n(\cdot)$. So the unknowns of (8) are $\mathbf{u}_H$, U_3 and P, all functions independent of z.

3.2 Analysis of the 2D horizontal problem

We are now interested in the well-posedness of (8). First of all, let us notice that

$$B(q, \mathbf{v}) = -\int_{\Sigma_F} \frac{h^2}{2} Q(div \mathbf{v}_H + V_3) dxdy, \quad \forall (\mathbf{v}, q) \in \mathbf{X}_H^0 \times M_H,$$

therefore :

$$\begin{array}{rcl} Ker_H B & = & \{\mathbf{v} \in \mathbf{X}_H^0;\ B(q, \mathbf{v}) = 0, \quad \forall q \in M_H\} \\ & = & \{\mathbf{v} \in \mathbf{X}_H^0;\ div \mathbf{v}_H + V_3 = 0 \text{ in } \Sigma_F\} \subset \mathbf{V}^0. \end{array}$$

This last inclusion together with $A_1(\mathbf{u}; \mathbf{u}, \mathbf{u}) = 0$ for any $\mathbf{u} \in \mathbf{X}_H^0$ yields the $\mathbf{X}-$coercivity of $A(\cdot;\cdot,\cdot)$ on $Ker_H B$, with the same coercivity constant as in 3D. Since $Ker_H B \subset \mathbf{V}^0$, the form $A_1(\cdot;\cdot,\mathbf{v})$ is sequentially weakly-continuous on $Ker_H B$ for all $\mathbf{v} \in Ker_H B$.

Then one only has to check the inf-sup condition, in order to get the existence of a solution of problem (8), by means of Brouwer's theorem (see the proof of Theorem 1). Since h vanishes on the lateral boundary Υ_{lat}, we use a technical result of [4] concerning the regularity of a degenerate elliptic problem in weighted Sobolev spaces, which we recall here below.

Lemma 1. *Suppose that Σ_F is a C^3 domain, $h \in W^{1,\infty}(\Sigma_F)$ and $h(x,y) = \varphi(dist((x,y), \partial\Sigma_F))$, where the function φ is a non decreasing Lipschitz function satisfying the conditions $\varphi(0) = 0$ and :*

$$\exists c > 0 \quad \textit{such that} \quad \forall s > 0,\ \left|\frac{\varphi'(s)}{\varphi(s)}\right| \leq \frac{c}{s},$$

$$\forall c_1, c_2 \in \mathbb{R}_+^*, \quad \exists C_1, C_2 \in \mathbb{R}_+^* \quad \textit{such that} \quad c_1 \leq \frac{s}{\tau} \leq c_2 \ \Rightarrow\ C_1 \leq \frac{\varphi(s)}{\varphi(\tau)} \leq C_2.$$

Let $\sqrt{h}f \in L^2(\Sigma_F)$. Then the solution of the boundary value problem :

$$\begin{cases} -div(\frac{1}{h}\nabla w) = f \quad in\ \Sigma_F \\ \frac{1}{h}\partial_n w = 0 \quad on\ \Upsilon_I \\ w = 0 \quad on\ \Upsilon_{lat} \end{cases} \tag{9}$$

has the following smoothness : $w \in H^1(\Sigma_F)$, $\frac{1}{\sqrt{h}}\nabla w \in \mathbf{L}^2(\Sigma_F)$, $\sqrt{h}\nabla(\frac{1}{h}\nabla w) \in \mathbf{L}^2(\Sigma_F)$. Moreover, the $L^2(\Sigma_F)$- norms of all these quantities are bounded by $\|f\|_{0,\Sigma_F,h}$, with a multiplicative constant depending only on the domain Σ_F.

Remark 2. *An example of such a function φ is $\varphi(s) = cs^\alpha$ with $c > 0$ and $0 < \alpha < 1$.*

Then one can establish :

Lemma 2. *Suppose the assumptions of Lemma 1 are fulfilled. Then the following inf-sup condition holds :*

$$\inf_{q\in M_H} \sup_{\mathbf{v}\in\mathbf{X}_H^0} \frac{B(q,\mathbf{v})}{\|\mathbf{v}\|_{\mathbf{X}} \|q\|_M} \geq c\sqrt{\Delta t}.$$

Proof. We apply again Fortin's trick. Let $q \in M_H$ and let us consider the auxiliary problem (9), with f replaced by $hQ \in L^2(\Sigma_F, h)$. We put $\mathbf{v}_H = \frac{1}{h}\nabla w$, $V_3 = 0$ and then we consider the 3D vector field $\mathbf{v} = (\mathbf{v}_H, \mathbf{v}_H \cdot \nabla Z_B + (z - Z_B)V_3)^t$. It is obvious that

$$B(q,\mathbf{v}) \quad = \quad \int_{\Sigma_F} \frac{h^3Q^2}{2} dxdy = \frac{3}{2}\|q\|_M^2 ,$$

while Lemma 1 gives that $\mathbf{v}_H \in \mathbf{H}^1(\Sigma_F, h)$. Thanks to the regularity of Z_B, one has that $v_B \in H^1(\Sigma_F, h)$ too and finally, that $\mathbf{v} \in \mathbf{H}^1(\Omega_F)$ with its norm bounded as follows :

$$\|\mathbf{v}\|_{1,\Omega_F} = \left(\|\mathbf{v}_H\|_{1,\Sigma_F,h}^2 + \|\mathbf{v}_H \cdot \nabla Z_B\|_{1,\Sigma_F,h}^2\right)^{1/2} \leq c\,\|hQ\|_{0,\Sigma_F,h} \leq c\,\|q\|_M .$$

By the trace theorem, we obtain that $\mathbf{v} \in \mathbf{X}_H^0$ and $\|\mathbf{v}\|_{\mathbf{X}} \leq \frac{c}{\sqrt{\Delta t}}\|q\|_M$, so the lemma is established with a constant c depending on Σ_F . □

In conclusion, one now obtains the existence of a solution to the nonlinear mixed problem (8); the uniqueness holds under the same hypothesis as in Theorem 1.

3.3 Comparison with the shallow water system

This subsection is devoted to the derivation of the 2D boundary value problem corresponding to the weak formulation (8), in order to compare it with the classical shallow water equations. For this purpose, we first write the forms $A_0(\cdot,\cdot)$, $A_1(\cdot;\cdot,\cdot)$ and $B(\cdot,\cdot)$ on the projection spaces and integrate with respect

to z. Then for any $\mathbf{u},\ \mathbf{v} \in \mathbf{X}_H^0$ and $p \in M_H^*,\ q \in M_H$ it follows that :

$$\begin{aligned}
A_0(\mathbf{u},\mathbf{v}) &= \int_{\Sigma_F} \frac{\rho h}{\Delta t}\left(\mathbf{u}_H\cdot\mathbf{v}_H + (u_B+\frac{h}{2}U_3)(v_B+\frac{h}{2}V_3) + \frac{h^2}{12}U_3V_3\right)dxdy \\
&+ \int_{\Sigma_F} \mu h\left(\frac{h^2}{12}\nabla U_3\cdot\nabla V_3 + curl\mathbf{u}_H\cdot curl\mathbf{v}_H\right)dxdy \\
&+ \int_{\Sigma_F} \mu h(\nabla u_B + \frac{h}{2}\nabla U_3 - U_3\nabla Z_B)\cdot(\nabla v_B + \frac{h}{2}\nabla V_3 - V_3\nabla Z_B)dxdy \\
&+ \int_{\Sigma_F} c_B\left(\mathbf{u}_H\cdot\mathbf{v}_H + u_Bv_B\right)\sqrt{1+|\nabla Z_B|^2}dxdy - \int_{\Sigma_F}\rho h f\mathbf{u}_H^{\perp}\cdot\mathbf{v}_H dxdy,
\end{aligned}$$

$$\begin{aligned}
A_1(\mathbf{u};\mathbf{u},\mathbf{v}) &= \int_{\Sigma_F}\rho h\left(curl\mathbf{u}_H\mathbf{u}_H^{\perp} - (u_B+\frac{h}{2}U_3)(\nabla u_B + \frac{h}{2}\nabla U_3 - U_3\nabla Z_B)\right)\cdot\mathbf{v}_H dxdy \\
&+ \int_{\Sigma_F}\rho h\left(\mathbf{u}_H\cdot(\nabla u_B + \frac{h}{2}\nabla U_3 - U_3\nabla Z_B)(v_B+\frac{h}{2}V_3) + \frac{h^2}{12}\mathbf{u}_H\cdot\nabla U_3V_3\right)dxdy \\
&- \int_{\Sigma_F}\rho\frac{h^3}{12}U_3\nabla U_3\cdot\mathbf{v}_H dxdy, \\
B(p,\mathbf{v}) &= -\int_{\Sigma_F}\frac{h^2}{2}Q(div\mathbf{v}_H + V_3)dxdy - \int_{\Sigma_F} hp_S(div\mathbf{v}_H + V_3)dxdy, \\
B(q,\mathbf{v}) &= -\int_{\Sigma_F}\frac{h^2}{2}Q(div\mathbf{v}_H + V_3)dxdy.
\end{aligned}$$

As regards the righthand-side term of (8), one gets that :

$$\begin{aligned}
F_H^n(\mathbf{v}) &= \int_{\Sigma_F}\frac{\rho h}{\Delta t}\left(\mathbf{u}_H^n\cdot\mathbf{v}_H + (u_B^n+\frac{h}{2}U_3^n)(v_B+\frac{h}{2}V_3) + \frac{h^2}{12}U_3^nV_3\right)dxdy \\
&- \int_{\Sigma_F}\rho hg(v_B+\frac{h}{2}V_3)dxdy + \int_{\Sigma_F} p_S(\mathbf{v}_H\cdot\nabla h - hV_3)dxdy \\
&+ \int_{\Sigma_F}\mathbf{w}\cdot\mathbf{v}\sqrt{1+|\nabla(Z_B+h)|^2}dxdy.
\end{aligned}$$

One can now deduce the interpretation of problem (8) in the sense of distributions. Thus, the 2D hydrodynamical model in the unknowns $(h,\mathbf{u}_H,U_3,P)$ is described by the following equation in Σ :

$$\frac{dh}{dt} - hU_3 = 0, \tag{10}$$

respectively the set of three equations in the domain $\Sigma_F(t)$ defined by $h>0$:

$$div\mathbf{u}_H + U_3 = 0, \tag{11}$$

$$\begin{aligned}
&h\left(\frac{\partial\mathbf{u}_H}{\partial t} + curl\mathbf{u}_H\mathbf{u}_H^{\perp}\right) + h\left(\frac{du_B}{dt} + \frac{h}{2}\frac{dU_3}{dt}\right)\nabla Z_B - h(u_B+\frac{h}{2}U_3)(\nabla u_B + \frac{h}{2}\nabla U_3 - U_3\nabla Z_B) \\
&-\frac{h^3}{12}U_3\nabla U_3 - hU_3u_B\nabla Z_B + \frac{\mu}{\rho}\mathbf{curl}(hcurl\mathbf{u}_H) - \frac{\mu}{\rho}div\left(h\nabla u_B + \frac{h^2}{2}\nabla U_3 - hU_3\nabla Z_B\right)\nabla Z_B \\
&+\frac{c_B}{\rho}\sqrt{1+|\nabla Z_B|^2}\left(\mathbf{u}_H + u_B\nabla Z_B\right) - hf\mathbf{u}_H^{\perp} + \tfrac{1}{\rho}\nabla(\frac{h^2}{2}P) = -gh\nabla Z_B + \mathbf{W},
\end{aligned} \tag{12}$$

$$\frac{h^2}{2}\frac{du_B}{dt} + \frac{h^3}{3}\frac{dU_3}{dt} - \frac{h^2}{2}U_3 u_B - \frac{\mu h}{\rho}\left(\nabla u_B + \frac{h}{2}\nabla U_3 - U_3\nabla Z_B\right)\cdot\nabla Z_B$$
$$-\frac{\mu}{\rho}div\left(\frac{h^2}{2}\nabla u_B + \frac{h^3}{3}\nabla U_3 - \frac{h^2}{2}U_3\nabla Z_B\right) - \frac{h^2}{2\rho}P = -\frac{h^2}{2}g + W_3, \quad (13)$$

where we have employed the notation

$$\frac{d\varphi}{dt} = \frac{\partial\varphi}{\partial t} + \mathbf{u}_H\cdot\nabla\varphi$$

for the total derivative of a scalar function $\varphi(t,x,y)$. The terms $\mathbf{W}$ and W_3 represent the wind's effects and are defined as follows :

$$\mathbf{W} = \frac{1}{\rho}\left((w_1,w_2)^t + w_3\nabla Z_B\right)\sqrt{1+|\nabla(Z_B+h)|^2},$$

$$W_3 = w_3 h\sqrt{1+|\nabla(Z_B+h)|^2}.$$

One still has to add initial conditions on h, $\mathbf{u}_H$ and U_3, as well as boundary conditions. The latter are deduced from the boundary integrals arising by integration by parts:

$$\int_{\partial\Sigma_F}\mu h\left(curl\mathbf{u}_H\mathbf{v}_H\cdot\mathbf{t}_H + v_B(\nabla u_B + \frac{h}{2}\nabla U_3 - U_3\nabla Z_B)\cdot\mathbf{n}_H\right)d\Gamma +$$
$$\int_{\partial\Sigma_F}\mu h V_3(\frac{h}{2}\nabla u_B + \frac{h^2}{3}\nabla U_3 - \frac{h}{2}U_3\nabla Z_B)\cdot\mathbf{n}_H d\Gamma$$
$$-\int_{\partial\Sigma_F}(\frac{h^2}{2}P + hp_S)\mathbf{v}_H\cdot\mathbf{n}_H d\Gamma = 0. \quad (14)$$

Finally, on Υ_{lat} (corresponding to the riverbanks) we have no boundary condition since $h=0$ while on Υ_I (corresponding to the inflow / outflow) we obtain:

$$\mathbf{u}_H\cdot\mathbf{n}_H = k_H,$$
$$curl\mathbf{u}_H - \frac{h}{6}\partial_n U_3\partial_t Z_B = 0,$$
$$\partial_n u_B + \frac{2h}{3}\partial_n U_3 - U_3\partial_n Z_B = 0.$$

■

Let us now consider the classical 2D shallow water equations. They are obtained from the incompressible 3D Navier-Stokes equations by neglecting the vertical velocity u_3 and by integrating the equations over the depth. This leads to a hydrostatic pressure :

$$p = p_S + \rho g(Z_B + h - z)$$

and to the following equations :

$$\frac{\partial h}{\partial t} + div\,(h\mathbf{u}_m) = 0, \quad (15)$$

$$\frac{\partial(h\mathbf{u}_m)}{\partial t} + div(h\mathbf{u}_m\otimes\mathbf{u}_m) - \gamma\Delta(h\mathbf{u}_m) + gh\mathbf{J} - hf\mathbf{u}_m^{\perp}$$
$$= -gh\nabla(Z_B+h) + \tilde{\mathbf{W}}, \quad (16)$$

where $\mathbf{u}_m = (u_{1m}, u_{2m})$ represents an averaged 2D velocity :

$$u_{im}(x,y,t) = \frac{1}{h}\int_{Z_B}^{Z_B+h} u_i dz, \quad i = 1,2.$$

The last term of (16) represents the wind's effect, γ is a viscosity coefficient (that certain models do not take into account) and $\mathbf{J}$ models the friction on the bottom. In practice, several formulae for $\mathbf{J}$ are available (Manning-Strickler, Chézy etc.) but none of them is rigourously justified from a mathematical point of view.

We are next interested in the comparison between our 2D model given by (10) - (13) and the shallow water system (15) - (16). We first note that one can easily eliminate U_3 from the relations (10) and (11) and thus get for our 2D model the same continuity equation as (15), with $\mathbf{u}_H$ playing the role of $\mathbf{u}_m$. As regards the momentum conservation law, in order to get a meaningful comparison, let us place ourselves in the same framework as for the shallow water equations. This translates into no vertical velocity and hydrostatic pressure. By imposing $u_B = U_3 = 0$, $P = \rho g$ and by neglecting the equations (11) and (13) associated with u_3 and P, our momentum law reduces to :

$$h\left(\frac{\partial \mathbf{u}_H}{\partial t} + curl\mathbf{u}_H\mathbf{u}_H^{\perp}\right) + \frac{\mu}{\rho}\mathbf{curl}(hcurl\mathbf{u}_H) + \frac{c_B}{\rho}\sqrt{1+|\nabla Z_B|^2}\mathbf{u}_H - hf\mathbf{u}_H^{\perp} = -gh\nabla(Z_B+h) + \mathbf{W}.$$

By means of the relation :

$$\mathbf{u}_H\cdot\nabla\mathbf{u}_H \quad = \quad curl\mathbf{u}_H\mathbf{u}_H^{\perp} + \frac{1}{2}\nabla(\mathbf{u}_H\cdot\mathbf{u}_H)$$

and by making use of the continuity equation, one can finally put the previous momentum equation under the following equivalent form :

$$\frac{\partial(h\mathbf{u}_H)}{\partial t} + div\,(h\mathbf{u}_H\otimes\mathbf{u}_H) + \frac{\mu}{\rho}\mathbf{curl}(hcurl\mathbf{u}_H) - \tfrac{h}{2}\nabla|\mathbf{u}_H|^2 + \frac{c_B}{\rho}\sqrt{1+|\nabla Z_B|^2}\mathbf{u}_H - hf\mathbf{u}_H^{\perp} = -gh\nabla(Z_B+h) + \mathbf{W}.$$

To conclude, one may note that Saint-Venant's equation (16) and ours are governed by the same main differential operators, but they differ through the diffusion and the friction terms (those who are in fact controversial in the derivation of the shallow water system). Since we are working with the dynamic pressure, we also have an additional correction term corresponding to $\rho|\mathbf{u}|^2$. An important point is that our approach avoids any closure problem.

Finally, let us note that several types of hydrodynamical models can be derived, depending on the choice of the time discretization and of the projection spaces $\mathbf{X}_H$ and M_H. For instance, one can employ the characteristics method and thus get linear time-discretized models and / or look for vertical velocity and pressure which are constant with respect to z instead of affine.

We refer to [2] for another variant of a 2D horizontal model. Its main advantages are a simpler description of the vertical velocity and hence a lower computational cost, as well as a closer comparison with the shallow water equations. Its main drawback is the fact that one can no longer derive a 1D model as a conforming approximation of the latter 2D model.

3.4 The non degenerate case

One may note that the hypotheses of Lemma 1 concerning the river's geometry are rather restrictive, at least as regards the regularity of Σ_F. Indeed, in view of the finite element discretization, the domain Σ_F will be further supposed to be polygonal.

Therefore, in what follows we consider the case where the water's depth is strictly positive ($h \geq h_{min} > 0$), corresponding to the presence of cliffs. We next discuss the modifications that this assumption implies, under the hypothesis $h \in W^{1,\infty}(\Sigma_F)$.

First, one may note that the projection of the free surface $\Gamma_S(t)$ on Σ does no more depend on time, so the computational domain Σ_F is always the same. However, the riverbed Γ_B now consists of three parts : the bottom, described by $z = Z_B(x,y)$ for $(x,y) \in \Sigma_F$, and two vertical lateral boundaries, described by $(x,y) \in \Upsilon_{lat}$.

Second, it is no longer necessary to work in weighted spaces, since the projection spaces can now be simply written as follows :

$$\begin{aligned} M_H &= \left\{q;\ q(x,y,z) = (Z_B + h - z)Q(x,y);\ Q \in L^2(\Sigma_F)\right\}, \\ \mathbf{X}_H &= \left\{(\mathbf{v}_H, v_3)^t;\ \mathbf{v}_H \in \mathbf{H}(div, curl; \Sigma_F),\ \ v_B \in H^1(\Sigma_F),\ V_3 \in H^1(\Sigma_F)\right\}, \\ \mathbf{X}_H^0 &= \left\{\ \mathbf{v} \in \mathbf{X}_H;\ \mathbf{v}_H \cdot \mathbf{n}_H = 0 \text{ on } \partial\Sigma_F\right\}. \end{aligned}$$

Consequently, the proof of the inf-sup condition stated in Lemma 2 necessitates less regularity for h and Σ_F. One can then establish :

Lemma 3. *Suppose that $0 < h_{min} \leq h \leq h_{max}$ and that Σ_F is a Lipschitz domain. Then the following inf-sup condition holds :*

$$\inf_{q \in M_H} \sup_{\mathbf{v} \in \mathbf{X}_H^0} \frac{B(q,\mathbf{v})}{\|\mathbf{v}\|_{\mathbf{X}} \|q\|_M} \geq c\sqrt{\Delta t}.$$

Proof. The proof makes use of Fortin's trick. For a given $q = (Z_B + h - z)Q \in M_H$, it is well-known (cf. [10]) that there exists $\mathbf{v}_H \in \mathbf{H}_0^1(\Sigma_F)$ such that

$$-div\mathbf{v}_H = hQ - \frac{1}{|\Sigma_F|}\int_{\Sigma_F} hQdxdy \quad \text{in } \Sigma_F.$$

We put $V_3 = -\frac{1}{|\Sigma_F|}\int_{\Sigma_F} hQdxdy$ and we define the operator $\mathcal{R}q = (\mathbf{v}_H, \mathbf{v}_H \cdot \nabla Z_B + (z - Z_B)V_3)^t$. It is then obvious to check that $\mathcal{R} : M_H \to \mathbf{X}_H^0$ satisfies :

$$\begin{aligned} B(q,\mathcal{R}q) &= \frac{1}{2}\int_{\Sigma_F} h^3Q^2dxdy = \frac{3}{2}\|q\|_M^2, \\ \|\mathbf{v}\|_{0,\Omega_F} + \|div\mathbf{v}\|_{0,\Omega_F} + \|\mathbf{curl}\mathbf{v}\|_{0,\Omega_F} + \|\mathbf{v}\|_{0,\Gamma_B} &\leq c\sqrt{h_{max}}\,\|hQ\|_{0,\Sigma_F} \leq c\sqrt{\frac{h_{max}}{h_{min}}}\,\|q\|_M \end{aligned}$$

which implies $\|\mathcal{R}q\|_{\mathbf{X}} \leq \frac{c}{\sqrt{\Delta t}}\|q\|_M$. So the announced inf-sup condition holds, with a constant c proportional to $\sqrt{\frac{h_{min}}{h_{max}}}$ and depending on the domain Σ_F. □

Finally, another difference between the degenerate and the non-degenerate cases concerns the boundary conditions satisfied by $\mathbf{u}_H$ and U_3 on Υ_{lat}. One

already has by construction that $\mathbf{u}_H \cdot \mathbf{n}_H = 0$, which ensures that $\mathbf{X}_H^0 \subset \mathbf{X}^0$, to which we add according to (14) :

$$curl\mathbf{u}_H - \frac{h}{6}\partial_n U_3 \partial_t Z_B = 0,$$
$$\partial_n u_B + \frac{2h}{3}\partial_n U_3 - U_3 \partial_n Z_B = 0.$$

4 Finite element approximation of the 2D model

We are now interested in the finite element approximation of the 2D horizontal model (10) - (13) in the non-degenerate case, on a polygonal domain Σ_F. So from now on, we assume that h is bounded from above by h_{max}, respectively from below by h_{min} where h_{min} and h_{max} are strictly positive constants.

Let $(\mathcal{T}_d)_{d>0}$ be a regular family of triangulations of Σ_F, each $\mathcal{T}_d$ consisting of triangles K such that $\overline{\Sigma}_F = \cup_{K\in\mathcal{T}_d}\overline{K}$. We first write the continuity equation as in (15) and then we time-discretize it as follows :

$$\frac{h - h^n}{\Delta t} + div(h\mathbf{u}_H^n) = 0.$$

The space discretization is achieved by means of a vertex-centered finite volume scheme, combined with a mass lumping technique. The height of water h is approximated by piecewise linear elements on each $K \in \mathcal{T}_d$, continuous on Σ_F.

Remark 3. *An alternative is to solve the continuity equation (15) by means of a cell-centered finite volume scheme, which yields a piecewise constant approximation of h, and to reconstruct the gradient of h in $F_d^n(\cdot)$ by post-processing.* ■

Concerning the time-discretized weak problem (8), our aim is to propose a low-order conforming approximation, such that both the discrete inf-sup condition on $B(\cdot,\cdot)$ and the coercivity of $A_0(\cdot,\cdot)$ on the discrete kernel of $B(\cdot,\cdot)$ be checked, uniformly with respect to the discretization parameter d. This last condition is crucial in order to derive optimal error bounds.

For this purpose, we introduce the finite dimensional spaces :

$$\begin{aligned}\mathbf{X}_d &= \left\{\mathbf{v}\in\mathbf{X}_H;\ (\mathbf{v}_H, V_3)^t \in \mathbf{H}^1(\Sigma_F),\ \forall K\in\mathcal{T}_d,\ (\mathbf{v}_H)_{/K}\in\mathbf{P}_1,\ (V_3)_{/K}\in P_1\oplus B_K\right\},\\ M_d &= \left\{q\in M_H;\ \forall K\in\mathcal{T}_d,\ Q_{/K}\in P_0\right\}\end{aligned}$$

as well as :

$$\mathbf{X}_d^* = \{\mathbf{v}\in\mathbf{X}_d;\ \mathbf{v}_H\cdot\mathbf{n}_H = k_d \text{ on } \Upsilon_I\ \},\quad \mathbf{X}_d^0 = \mathbf{X}_H^0\cap\mathbf{X}_d$$

where k_d is a P_1- continuous approximation of the data k_H on Υ_I. Here above, $B_K = span\{b_K\}$ is the space of bubble functions on K, with $b_K = \lambda_1\lambda_2\lambda_3$ and $\{\lambda_i\}_{1\le i\le 3}$ the barycentric coordinates of the triangle K. We also substitute h in $B(\cdot,\cdot)$ by its L^2- orthogonal projection h^* on M_d.

Then we solve, at each time-step, the following discrete problem :

$$\left\{\begin{array}{l} Find\ (\mathbf{u}_d, p_d)\in\mathbf{X}_d^*\times M_d\\ \forall\mathbf{v}\in\mathbf{X}_d^0,\quad A(\mathbf{u}_d;\mathbf{u}_d,\mathbf{v}) + B_d(p_d,\mathbf{v}) = F_d^n(\mathbf{v})\\ \forall q\in M_d,\quad B_d(q,\mathbf{u}_d) = 0,\end{array}\right. \tag{17}$$

where $F_d^n(\cdot)$ is obtained from $F_H^n(\cdot)$ by replacing $\mathbf{u}_{2D}^n$ by $\mathbf{u}_d^n$ and where the new bilinear form $B_d(\cdot,\cdot)$ is defined by :

$$B_d(q,\mathbf{v}) = -\frac{1}{2}\int_{\Sigma_F} (h^*)^2 Q(div\mathbf{v}_H + V_3)dxdy, \quad \forall (q,\mathbf{v}) \in M_d \times \mathbf{X}_d^0.$$

In order to prove the well-posedness of (17), let us first establish a preliminary result, which will allow us to replace the weight h by h^* in the norms $\|\cdot\|_{\mathbf{X}}$ and $\|\cdot\|_M$ on the discrete spaces $\mathbf{X}_d^0$ and M_d.

Lemma 4. *Let any $K \in \mathcal{T}_d$ and let $\mathcal{P}$ be a given polynomial space on K. Then there exist $c_1,\ c_2 > 0$ independent of h and K such that :*

$$\forall v \in \mathcal{P}, \quad c_1 \int_K h\,|v|\,dxdy \le \int_K h^*\,|v|\,dxdy \le c_2 \int_K h\,|v|\,dxdy.$$

Proof. We recall that h is linear and strictly positive on K, whereas $h^* = \frac{1}{|K|}\int_K h dxdy$ is a strictly positive constant. Let us define on $\mathcal{P}$ the applications $N_1,\ N_2$ by :

$$N_1(v) = \int_K h\,|v|\,dxdy, \quad N_2(v) = (\int_K h dxdy)(\int_K |v|\,dxdy), \quad \forall v \in \mathcal{P}.$$

Obviously, N_1 and N_2 are two norms, equivalent on the finite dimensional space $\mathcal{P}$. By means of a classical passage to the reference element, we deduce that there exist two constants, depending *a priori* on h but independent of the size of K, such that :

$$\forall v \in \mathcal{P}, \quad c_1(h) \int_K h\,|v|\,dxdy \le \frac{1}{|K|}(\int_K h dxdy)(\int_K |v|\,dxdy) \le c_2(h) \int_K h\,|v|\,dxdy.$$

We still have to prove that c_1, c_2 are independent of h. For this purpose, we write that $h = \sum_{i=1}^3 h(N_i)\lambda_i$ where $h(N_i)$ are the values of h at the nodes N_i belonging to K. Since λ_i are positive on K, the previous relation holds if one substitutes h by λ_i, for $1 \le i \le 3$. Then the conclusion follows thanks to the fact that $h(N_i) \ge 0$, with $c_1 = \min_{1\le i\le 3} c(\lambda_i)$ and $c_2 = \max_{1\le i\le 3} c(\lambda_i)$. □

Remark 4. *A similar result holds when replacing h and h^* by h^α and $(h^*)^\alpha$ respectively, for a given $\alpha \in \mathbb{N}^*$. Indeed, in this case one can put $N_1(v) = \int_K h^\alpha\,|v|\,dxdy$, $N_2(v) = (\int_K h^\alpha dxdy)(\int_K |v|\,dxdy)$ and obtain, as in the proof above, that :*

$$\forall v \in \mathcal{P}, \quad c_1 \int_K h^\alpha\,|v|\,dxdy \le \frac{1}{|K|}(\int_K h^\alpha dxdy)(\int_K |v|\,dxdy) \le c_2 \int_K h^\alpha\,|v|\,dxdy.$$

The desired result follows due to the equivalence between $(\sum_{i=1}^3 h(N_i))^\alpha$ and $\sum_{i=1}^3 h(N_i)^\alpha$, which implies the equivalence between $\int_K h^\alpha dxdy$ and $\int_K (h^*)^\alpha dxdy$.

In order to prove the well-posedness of the discrete problem, we assume in what follows that

$$\exists \sigma_0, \sigma_1 > 0 \text{ s.t. } \forall K \in \mathcal{T}_d, \quad \sigma_0 \le \frac{h_K^*}{|K|^{1/2}} \le \sigma_1. \tag{18}$$

Remark 5. *One can associate with the 2D triangulation $\mathcal{T}_d$ a 3D one, denoted by $\mathcal{T}_{3D}$ and consisting of one layer of prisms (of basis $K \in \mathcal{T}_d$ and height h_K^*). Then the assumption (18) translates the fact that $\mathcal{T}_{3D}$ is regular (in the sense of Ciarlet). So (18) is not a restrictive hypothesis, since a 2D approximation of a river flow is usually derived under the shallow water assumption (i.e. the height of water is supposed to be small with respect to the other dimensions of the river).*

We are now able to establish :

Theorem 3. *Under the hypothesis (18), the nonlinear problem (17) has a unique solution.*

Proof. The proof relies on the discrete inf-sup condition on $B_d(\cdot,\cdot)$ and the coercivity of $A(\cdot;\cdot,\cdot)$ on

$$Ker_d B \quad = \quad \left\{ \mathbf{v} \in \mathbf{X}_d^0;\ \forall K \in \mathcal{T}_d,\ \int_K (div\mathbf{v}_H + V_3) dxdy = 0 \right\}.$$

We first prove that there exists $c > 0$ independent of h and of the discretisation such that

$$A(\mathbf{v};\mathbf{v},\mathbf{v}) \geq c \left\|\mathbf{v}\right\|_{\mathbf{X}}^2, \quad \forall \mathbf{v} \in Ker_d B. \tag{19}$$

Since $A_1(\mathbf{v};\mathbf{v},\mathbf{v}) = 0$ for any $\mathbf{v} \in \mathbf{X}_H^0$ and since $\mathbf{X}_d^0 \subset \mathbf{X}_H^0$, we only have to prove the uniform coercivity of $A_0(\cdot,\cdot)$ on $Ker_d B$ in order to obtain the previous assertion. Note that $Ker_d B \nsubseteq Ker_{2D} B$. So let $\mathbf{v} \in Ker_d B$ and let us bound the term $\int_{\Sigma_F} h(div\mathbf{v}_H + V_3)^2 dxdy$. One has on a given triangle $K \in \mathcal{T}_d$ that $div\mathbf{v}_H = -\frac{1}{|K|}\int_K V_3 dxdy = -V_3^*$, therefore :

$$\int_K h^*(div\mathbf{v}_H + V_3)^2 dxdy = h_K^* \left\|V_3 - V_3^*\right\|_{0,K}^2 \leq c h_K^* \left|K\right| \left|V_3\right|_{1,K}^2 \leq c\sigma_0 (h_K^*)^3 \left|V_3\right|_{1,K}^2.$$

By summing upon all the triangles of $\mathcal{T}_d$, one then gets :

$$\int_{\Sigma_F} h(div\mathbf{v}_H + V_3)^2 dxdy \leq c \left\|\mathbf{curlv}\right\|_{0,\Omega_F}^2, \quad \forall \mathbf{v} \in Ker_d B$$

so the statement (19) is established.

We now turn to the bilinear form $B_d(\cdot,\cdot)$ and prove that there exists $c > 0$ independent of h and of the discretisation such that :

$$\inf_{q \in M_d} \sup_{\mathbf{v} \in \mathbf{X}_d^0} \frac{B_d(q,\mathbf{v})}{\left\|\mathbf{v}\right\|_{\mathbf{X}} \left\|q\right\|_M} \geq c\sqrt{\Delta t}. \tag{20}$$

The proof is based on Fortin's trick and on the continuous inf-sup condition. Let any $q \in M_d$. Then one has, according to the Remark 4, that

$$c_1 \int_{\Sigma_F} h^3 Q^2 dxdy \leq \int_{\Sigma_F} (h^*)^3 Q^2 dxdy \leq c_2 \int_{\Sigma_F} h^3 Q^2 dxdy,$$

hence $h^*Q \in L^2(\Sigma_F, h)$ and the norms $\left\|h^*Q\right\|_{0,\Sigma_F,h}$ and $\left\|q\right\|_M$ are equivalent. Following the proof of Lemma 3, we then associate with h^*Q a function $\mathbf{v} \in \mathbf{X}_{2D}^0$ satisfying $div\mathbf{v}_H + V_3 = -h^*Q$ and :

$$\begin{aligned} \left\|\mathbf{v}\right\|_{0,\Omega_F} + \left\|div\mathbf{v}\right\|_{0,\Omega_F} + \left\|\mathbf{curlv}\right\|_{0,\Omega_F} + \left\|\mathbf{v}\right\|_{0,\Gamma_B} \quad &\leq c\sqrt{\frac{h_{max}}{h_{min}}} \left\|q\right\|_M, \\ B_d(q,\mathbf{v}) = \tfrac{1}{2}\int_{\Sigma_F} (h^*)^3 Q^2 dxdy = \tfrac{3}{2} \left\|q\right\|_M^2. \end{aligned}$$

We next construct a couple of discrete functions $(\mathbf{v}_H^d, V_3^d)$ as follows : $\mathbf{v}_H^d$ is the Clément interpolate (cf. [6]) of the previous $\mathbf{v}_H$ and

$$\forall K \in \mathcal{T}_d, \quad (V_3^d)_{/K} = \alpha_K b_K \quad \text{with} \quad \alpha_K = \frac{\int_K div(\mathbf{v}_H - \mathbf{v}_H^d) dxdy}{\int_K b_K dxdy}.$$

This choice ensures that the corresponding 3D function $\mathbf{v}^d$ belongs to $\mathbf{X}_d^0$ and moreover, that $B_d(q, \mathbf{v}^d) = B_d(q, \mathbf{v})$ since h^* and Q are piecewise constant and :

$$\int_K (div\mathbf{v}_H^d + V_3^d) dxdy \quad = \quad \int_K div\mathbf{v}_H dxdy = -\int_K h^* Q dxdy.$$

We still have to prove that $\left\|\mathbf{v}^d\right\|_{\mathbf{X}} \leq \frac{c}{\sqrt{\triangle t}} \|q\|_M$ in order to etablish (20). According to the relations (7), it is sufficient to bound the following terms : $\int_{\Sigma_F} \left|\mathbf{v}_H^d\right|^2 dxdy$, $\int_{\Sigma_F} h \left|\mathbf{v}_H^d\right|^2 dxdy$, $\int_{\Sigma_F} h \left|\nabla \mathbf{v}_H^d\right|^2 dxdy$, $\int_{\Sigma_F} h^3 (V_3^d)^2 dxdy$, $\int_{\Sigma_F} h^3 \left|\nabla V_3^d\right|^2 dxdy$ and $\int_{\Sigma_F} h (div\mathbf{v}_H^d + V_3^d)^2 dxdy$. Thanks to Lemma 4, we can replace h by h^* in all the previous terms. According to [6], the following estimates hold on every $K \in \mathcal{T}_d$:

$$\begin{aligned} \left\|\mathbf{v}_H - \mathbf{v}_H^d\right\|_{0,K} &\leq c \|\mathbf{v}_H\|_{0,\Delta}, \\ \left\|\nabla(\mathbf{v}_H - \mathbf{v}_H^d)\right\|_{0,K} &\leq c \|\nabla \mathbf{v}_H\|_{0,\Delta} \end{aligned}$$

where $\Delta = \left\{K' \in \mathcal{T}_d;\ \overline{K'} \cap \overline{K} \neq \emptyset\right\}$. Note that the assumption (18) implies that there exists $c > 0$ such that :

$$\forall K, K' \quad \in \quad \mathcal{T}_d \text{ with } \overline{K'} \cap \overline{K} \neq \emptyset \ : \quad h_K^* \leq c h_{K'}^*. \tag{21}$$

Therefore, by means of the triangle inequality and by using (21), one obtains that :

$$\begin{aligned} &\tfrac{1}{\triangle t} \int_{\Sigma_F} h^* \left|\mathbf{v}_H^d\right|^2 dxdy + \int_{\Sigma_F} h^* \left|\nabla \mathbf{v}_H^d\right|^2 dxdy + \int_{\Sigma_F} \left|\mathbf{v}_H^d\right|^2 dxdy \\ &\leq c(\tfrac{1}{\triangle t} \int_{\Sigma_F} h^* \left|\mathbf{v}_H\right|^2 dxdy + \int_{\Sigma_F} h^* \left|\nabla \mathbf{v}_H\right|^2 dxdy + \int_{\Sigma_F} \left|\mathbf{v}_H\right|^2 dxdy) \\ &\leq \tfrac{c}{\triangle t} \|q\|_M^2 \end{aligned}$$

where the constant c is proportional to $\frac{h_{max}}{h_{min}}$. Reverting to the reference element, one next gets on every $K \in \mathcal{T}_d$ that :

$$\frac{1}{|K|} \int_K b_K^2 dxdy + \int_K \left|\nabla b_K\right|^2 dxdy \leq \frac{c}{|K|^2} (\int_K b_K dxdy)^2.$$

Together with (21) and the estimate

$$\left| \int_K div(\mathbf{v}_H - \mathbf{v}_H^d) dxdy \right| \leq c |K|^{1/2} \|\nabla \mathbf{v}_H\|_{0,\triangle},$$

this finally yields :

$$\begin{aligned} \int_K (h^*)^3 (V_3^d)^2 dxdy &\leq c (h_K^*)^3 \|\nabla \mathbf{v}_H\|_{0,\triangle}^2 \leq c \int_\triangle h^* \left|\nabla \mathbf{v}_H\right|^2 dxdy, \\ \int_K (h^*)^3 \left|\nabla V_3^d\right|^2 dxdy &\leq c \frac{(h_K^*)^3}{|K|} \|\nabla \mathbf{v}_H\|_{0,\triangle}^2 \leq c \frac{(h_K^*)^2}{|K|} \int_\triangle h^* \left|\nabla \mathbf{v}_H\right|^2 dxdy. \end{aligned}$$

We can now conclude to (20) thanks to the assumption (18), where the constant c of the inf-sup condition is proportional to $\sqrt{\frac{h_{min}}{h_{max}}}$.

Finally, Brouwer's theorem together with the properties (19) and (20) yield the well-posedness of the discrete problem (17). □

Remark 6. *Due to the similarity between our form $B(\cdot,\cdot)$ and that of the 2D Stokes problem on Σ_F :*

$$b_S(Q_S, \mathbf{v}_S) \quad = \quad -\int_{\Sigma_F} Q_S div \mathbf{v}_S dxdy, \quad \forall (Q_S, \mathbf{v}_S) \in L^2_0(\Sigma_F) \times \mathbf{H}^1_0(\Sigma_F),$$

one may note that it is also possible to employ P_0- elements for the pressure and continuous$\mathbf{P}_2$- elements for the horizontal velocity, whereas the vertical velocity can be classically approximated by continuous P_1- elements. This choice ensures the well-posedness of the discrete problem without any additional assumption on the triangulation (cf. for instance [10]) but it is more expensive from a computational point of view.

Remark 7. *One may also treat the degenerate case, which notably allows one to treat flood problems. For this purpose, let $(\mathcal{T}_d)_{d>0}$ be a regular family of triangulations of Σ; the computational domain Σ^{n+1} is then defined as the set of triangles of $\mathcal{T}_d$ on which h is positive and has at least one strictly positive vertex value. Since $h^* > 0$ on Σ^{n+1}, all the previous results of this section hold, but the constant of the inf-sup condition for $B(\cdot,\cdot)$ now depends on h^*_{min}.*

5 Numerical results

5.1 Comparison with the shallow water system

We begin by presenting some comparisons between the previous 2D horizontal model and the classical shallow water equations, where a Manning-Strickler friction term as well as a viscosity term ($\mu = 10^{-6}$) are considered.

The comparisons are performed on three academic configurations, depending on the river's geometry : a flat bottom rectilinear channel, a flat bottom nonrectilinear channel and finally a rectilinear channel with varying topography. A description of the geometries and meshes of the free surface for the three cases is given in Figure 1. Note that same mesh and same time-step ($\Delta t = 0,5s$) were used for both the shallow water model and ours. For all these examples, an inflow condition is imposed on the left boundary whereas an outflow condition is set on the right boundary. The initial elevation is about 6 meters and the initial velocity is null.

As expected, one may notice that the evolution in time of the water's height is very similar for the two models, in all considered cases (see Figure 2). One also obtains close results for the horizontal velocities, as shown in Figure 3 for the case of a nonrectilinear channel. However, our model provides a more accurate representation of the 3D velocity. We have reconstructed in Figure 4 the velocity field computed by the two models in the longitudinal plane (u_1, u_3). One can see that the vertical component u_3 (which is zero in the shallow water model) is actually non negligeable, especially close to the variations of the bottom and of the free surface.

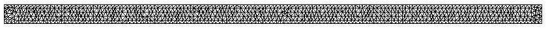

(a) Flat bottom rectilinear channel (1500m x 50m)

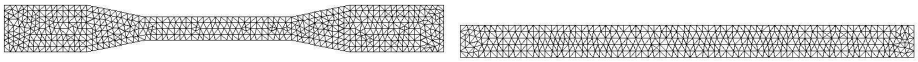

(b) Flat bottom nonrect. channel (150m x 80m)

(c) Rect. channel with varying bottom (750m x 50m)

Figure 1: Academic test-cases : geometry and triangulation of the free surface

(a) Flat bottom rectilinear channel

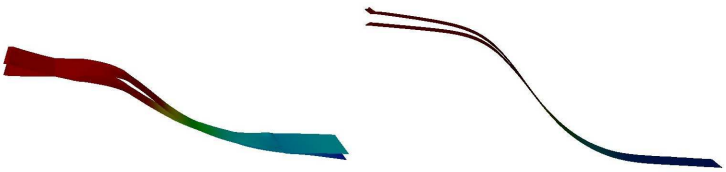

(b) Flat bottom nonrectilinear channel

(c) Rectilinear channel with varying bottom

Figure 2: Height of water : comparison between shallow water and new model

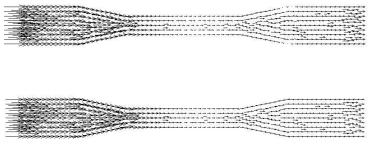

Figure 3: Flat bottom nonrectilinear channel : comparison of horizontal velocity fields

5.2 More realistic tests

This subsection is devoted to realistic simulations of the hydrodynamics of the Adour river, situated in the south-west of France (see Figure 5 for its geometry). In the examples presented below, the real bathymetry as well as measured

(a) Geometry of the bottom

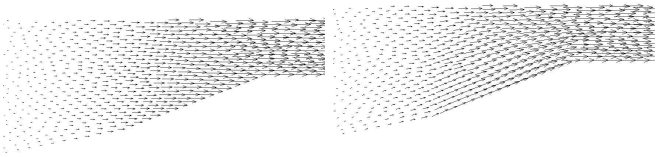

(b) Shallow water model (c) New model

Figure 4: Rectilinear channel with varying bottom : comparison of velocity fields in the longitudinal plane

flowrates on the inflow and outflow boundaries are employed. Moreover, the simulations are achieved with tide coefficients computed using the moon's cycle and allowing us to impose the height of the water on the estuarine boundary. All the previous data were provided by IFREMER[1].

In order to validate the developed code, we next present three examples of comparison between the velocities computed by our 2D model and those measured by IFREMER, by means of two current meters located at different depths : one close to the free surface and the other 1 meter below. In the first two examples, the measurements were performed during several short periods of time (of about 10 minutes each), while in the last example they were taken during a longer period (about 1h30′).

First, the measurements were carried out at the point indicated in Figure 7 (a), where one can also see the horizontal velocity field given by our code at a given time step. In Figure 7 (b), we have represented the evolution in time of the computed velocity's magnitude versus the measured one, which is averaged with respect to time and is represented by horizontal lines, at different moments. The dotted curve A corresponds to the result of a 1D shallow water code previously employed by IFREMER, whereas the three other curves (B, C and D respectively) correspond to the results of our code on the upper riverbank, the lower riverbank and the median curve of the river respectively.

Second, the measurements were performed on the two riverbanks of the river, near the island represented in Figure 6 (b). In Figure 8 the flow is directed from the left to the right (corresponding to high tide) whereas in Figure 9 the flow has an opposite direction, corresponding to low tide. In the two cases, the measurements took place downstream (that is, on the righthand side of the island in Figure 8, respectively on the lefthand side in Figure 9), at the points indicated on each figure. On the one hand, Figures 8 (a) and 9 (a) present the horizontal velocity field and highlight the fact that the flow around the island is asymmetrical; thus, a 1D model couldn't be employed with success on this

[1]French Institute of Maritime Research

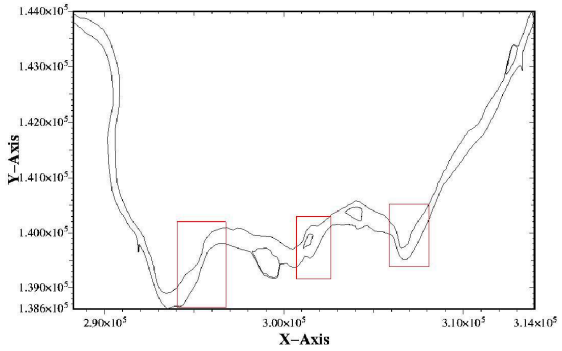

Figure 5: Geometry of the Adour river on 30km

zone of the river. On the other hand, we compare in Figures 8 (b) and 9 (b) the velocity's magnitude given by our code with that measured by IFREMER. The two curves show the evolution of the computed velocity near the upper, respectively the lower riverbank. We have also represented in Figure 9 (c) the evolution in time of the velocity computed by the 2D code (curves C and D), that given by the 1D shallow water code of IFREMER (curves A and B) and finally, the one measured during short periods (discontinuous horizontal lines), but now at the two points situated on the two branches of the river and indicated in Figure 9 (a); the red colour (curves B and D) corresponds to the lower branch and the blue one (curves A and C) to the upper branch.

The conclusion of the previous tests is that the 2D developed code gives a good approximation of the real velocity, even in the rather delicate case of flow around an island, while the 1D code provides quite poor results.

Third, the measurements were carried out in a fixed point, situated near the meander represented in Figure 6 (c), during 1h30′. We have represented in Figure 10 (b) the evolution in time of the velocity's magnitude at this point : curve C corresponds to the computed velocity, while the B and D curves correspond to the measurements. The dotted curve A represents the velocity's magnitude computed by the 1D shallow water code. Once again, one can observe that the 2D code closely reproduces the evolution of the real velocity; moreover, as expected near a meander, the 1D code fails to give good results. The velocity field at a given time step can also be seen in Figure 10 (a).

Finally, we present an example of flood simulation, emphasizing the fact that the code can equally be used in the case of a moving domain (see also Remark 7). We have simulated the overflow of an island by imposing large flowrates and a large tide coefficient. An adaptive time-step was used and as previously, we have employed real data except for the island's topography which was supposed to be flat, for the sake of simplicity. We have represented on the same figure the height of water and the velocity, at different time steps (see Figure 11). One can thus see that the island is completely submerged during the simulation and then unflooded at the end of the simulation; we don't dispose of measured data in order to validate this test-case.

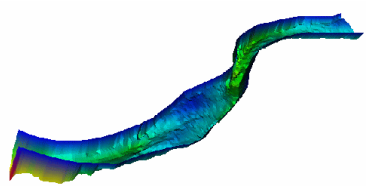

(a) The highway bridge

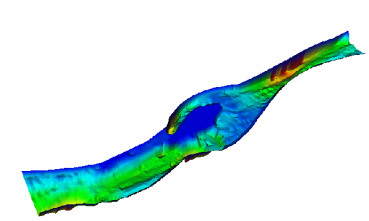

(b) The Broc island

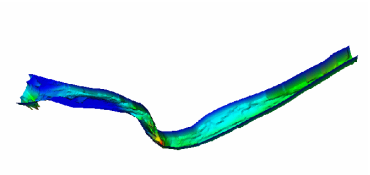

(c) The Urt meander

Figure 6: Bathymetry of the domains concerned by IFREMER measurements

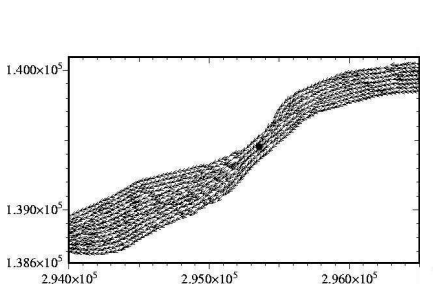

(a) Horizontal velocity field

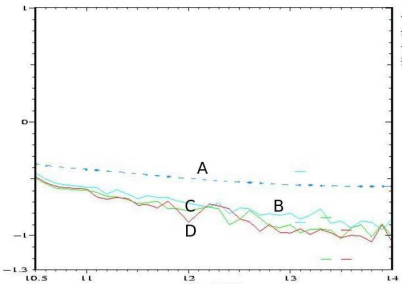

(b) Measurements vs computations

Figure 7: Flow near the highway bridge

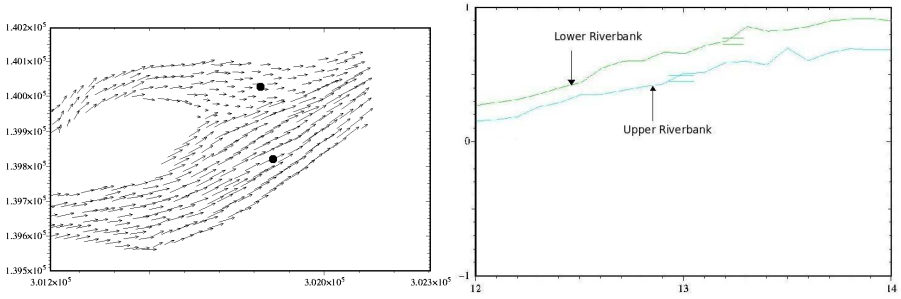

(a) Horizontal velocity field

(b) Comparison with measurements near riverbanks

Figure 8: The Broc island : flow oriented from left to right

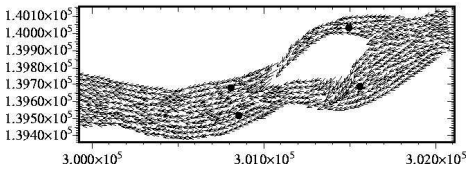

(a) Horizontal velocity field

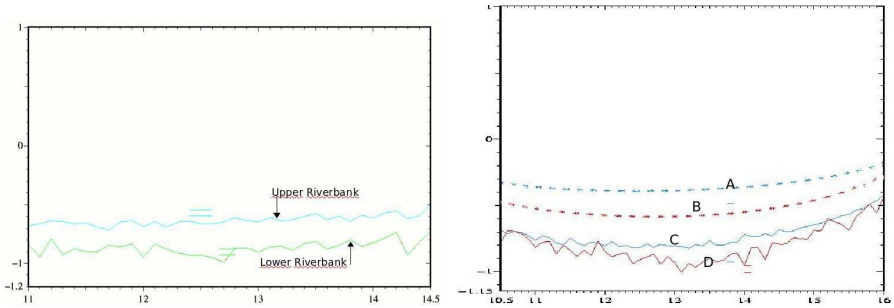

(b) Comparison with measurements near riverbanks

(c) Comparison with measurements on each branch

Figure 9: The Broc island : flow oriented from right to left

References

[1] V.I. Agoshkov, D. Ambrosi, V. Pennati, A. Quarteroni and F. Saleri, Mathematical and numerical modeling of shallow water flow, *Comput. Mech.* 11 (1993) 280-299.

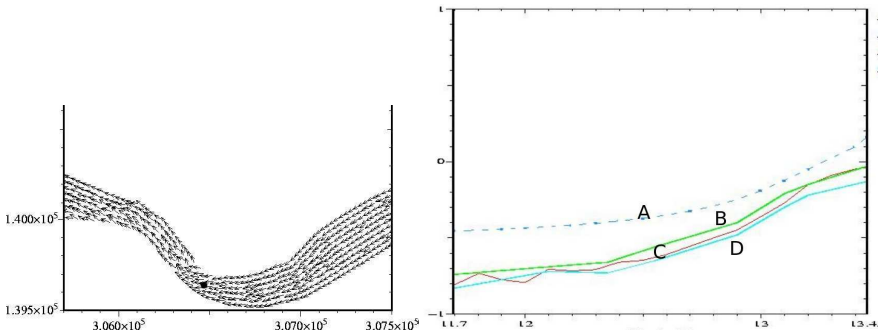

(a) Horizontal velocity field (b) Comparison with measurements during 1h30'

Figure 10: Flow at the Urt meander

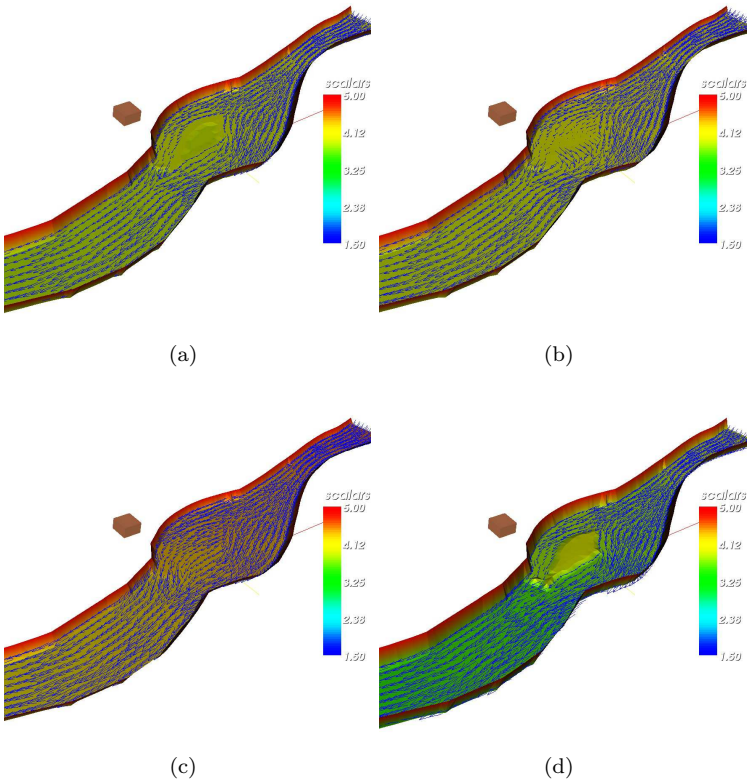

(a) (b)

(c) (d)

Figure 11: Flood simulation of the Broc island : water elevation and velocity field

[2] M. Amara, D. Capatina-Papaghiuc and D. Trujillo, *Modélisation 2D horizontale de l'écoulement d'un fleuve*, Preprint LMA 03/23, Université de Pau (2003) *(http://lma-umr5142.univ-pau.fr/live/Prepublications/Archives)*

[3] M. Amara, D. Capatina-Papaghiuc and D. Trujillo, Hydrodynamical modeling and multidimensional approximation of estuarian river flows, *Comput. Vis. Sci.*, vol. 6 (2004) 39-46.

[4] D. Bresch, F. Guillen and J. Lemoine, A note on a degenerate elliptic equation with applications for seas and lakes, *Elect. J. Diff. Eqs.*, vol. 42 (2004) 1-13

[5] F. Brezzi and M. Fortin, *Mixed and Hybrid Finite Element Methods,* Springer Verlag, New York (1991).

[6] P. Clément, Approximation by finite element functions using local regularization, *R.A.I.R.O. Anal. Numer.* 9 R2 (1975) 77-84.

[7] M. Costabel, A remark on the regularity of solutions of Maxwell's equations in Lipschitz domains, *Mathematical Methods in Applied Sciences*, vol. 12 (1990) 365-368.

[8] S. Ferrari and F. Saleri, A new two-dimensional shallow-water model including pressure effects and slow varying bottom topography, *M2AN*, vol. 38, n. 2 (2004) 211-234.

[9] J.-F. Gerbeau and B. Perthame, Derivation of Viscous Saint-Venant System for Laminar Shallow Water, Numerical Validation, *Discrete and Continuous Dynamical Systems*, Ser. B, vol. I, n. 1 (2001) 89-102.

[10] V. Girault and P.A. Raviart, *Finite Element Methods for Navier-Stokes Equations. Theory and Algorithms*, Springer Verlag, Berlin (1986).

[11] W.H. Graf, *Fluvial Hydraulics*, John Wiley & Sons, Chichester (1998).

[12] P. Grisvard, *Singularities in Boundary Value Problems*, Masson, Paris (1992).

Centre de recherche INRIA Bordeaux – Sud Ouest
Domaine Universitaire - 351, cours de la Libération - 33405 Talence Cedex (France)

Centre de recherche INRIA Grenoble – Rhône-Alpes : 655, avenue de l'Europe - 38334 Montbonnot Saint-Ismier
Centre de recherche INRIA Lille – Nord Europe : Parc Scientifique de la Haute Borne - 40, avenue Halley - 59650 Villeneuve d'Ascq
Centre de recherche INRIA Nancy – Grand Est : LORIA, Technopôle de Nancy-Brabois - Campus scientifique
615, rue du Jardin Botanique - BP 101 - 54602 Villers-lès-Nancy Cedex
Centre de recherche INRIA Paris – Rocquencourt : Domaine de Voluceau - Rocquencourt - BP 105 - 78153 Le Chesnay Cedex
Centre de recherche INRIA Rennes – Bretagne Atlantique : IRISA, Campus universitaire de Beaulieu - 35042 Rennes Cedex
Centre de recherche INRIA Saclay – Île-de-France : Parc Orsay Université - ZAC des Vignes : 4, rue Jacques Monod - 91893 Orsay Cedex
Centre de recherche INRIA Sophia Antipolis – Méditerranée : 2004, route des Lucioles - BP 93 - 06902 Sophia Antipolis Cedex

Éditeur
INRIA - Domaine de Voluceau - Rocquencourt, BP 105 - 78153 Le Chesnay Cedex (France)
http://www.inria.fr
ISSN 0249-6399